NASA
Technical
Paper
3432

November 1993

Total Systems Design Analysis of High Performance Structures

V. Verderaime

NASA

NASA Technical Paper 3432

1993

Total Systems Design Analysis of High Performance Structures

V. Verderaime
George C. Marshall Space Flight Center
Marshall Space Flight Center, Alabama

National Aeronautics and Space Administration
Office of Management
Scientific and Technical Information Program

ACKNOWLEDGMENTS

The author acknowledges Dr. J. Blair for this opportunity and his expressed interest in enhanced, reliable, and least-cost operations queried throughout the study. Suggestions by Dr. J. Blair, Mr. R. Ryan, Mr. M. Rheinfurth, and Dr. J. Brunty on presentation are appreciated. Gratitude is extended to NASA centers and associated industries, and especially to Chief Scientist J. Sobieski of Langley Research Center, for their valuable review comments. The author is thankful for Mrs. Rene McBrayer's invaluable administrative and logistic assistance.

TABLE OF CONTENTS

LIST OF ILLUSTRATIONS

TECHNICAL PAPER

TOTAL SYSTEMS DESIGN ANALYSIS OF HIGH PERFORMANCE STRUCTURES

I. INTRODUCTION

Competitive demands for reliable and affordable products elicit higher standards and innovative ways of designing complex systems. While design analysts are striving to reduce development and operational costs through robustness, streamlining, and automating methodologies within their respective disciplines, quality management between discipline interfaces is not equably practiced. The purpose of this study was to understand the flow and interactions between designing disciplines in order to identify, assess, and characterize interface designer control parameters that optimize and govern structural system performance. Performance is interacted and further optimized in parallel with development and life cycle events for a reliable, least-cost total system design.

System design is a multilevel, multidiscipline, integration, and iteration process. Improving performance models of physical realities rests with respective disciplines, but optimizing the total system of models and service events may be achieved through a cohesive design process that identifies and characterizes designer control parameters at multidiscipline interfaces. Accordingly, a matrix is proposed for sorting and tracking root interface tasks which consist of assessing sensitivities of interface input-output design parameters, characterizing statistical parameters, resolving deficiencies, optimizing designer controlled parameters with reliability and least cost, and updating and iterating sensitive interface parameters. Identified interfaces are accompanied by narratives defining each interface task. Tasks are processed through systems engineering design phases and in support of concurrent engineering roles.

Though the total system design analysis process is adaptable to most transportation systems, launch vehicle environments are primarily featured. An aerospace carrier mission consists of six concise systems with interacting requirements, constraints, and solutions, of which structures is the subject system. The structural system hierarchy leading to performance interfaces and life-cycle interactions is illustrated in figure 1. Structural environments and envelope sizes which initiate the design process are derived from all of the transportation interacting systems. Design downstream constraints are imposed by manufacturing, verification, and operational interactions and expectations.

As a system, the presentation flows down the matrix along performance disciplines denoting sections, and each text section develops interfaces and techniques leading to subsequent sections. It steps briefly through environments and materials properties and their integration with multidiscipline computational and design techniques in order to understand and optimize their intrinsic interactions and iterations through interface design parameters. As a total system, the process interacts latterly and simultaneously with development and operational interfaces and constraints for a total life-cycle design analysis. Interface optimization deficiencies and related issues in current practices are addressed.

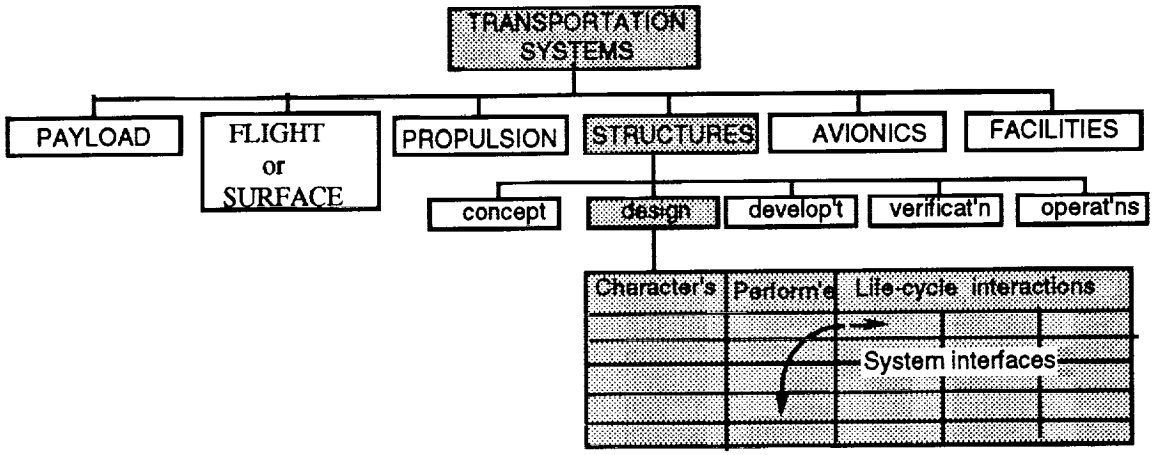

Figure 1. Structural system hierarchy.

A typical structural failure concept is presented which integrates loads, stress, and materials disciplines. Current reliability and deterministic techniques, benefits, and limitations are discussed. A system deterministic probability concept is proposed for semistatic structures which combines the benefits of the reliability and deterministic methods. Quality function design is briefly introduced to better fit design modes with changing environments.

No attempt was made to expound on conventional aspects of structural design, nor to elaborate on applied techniques and standards referenced here and amply documented elsewhere. Only minor supplements to current design practices and first-order adaptation of existing techniques were considered to facilitate implementation of promising results.

The presentation may be limited in detail, but it is broad in scope and application over a wide variety of structural systems in the transportation industry in general, and the aerospace enterprise in particular. It is hoped that the interested audience will improve, expand, and render a more practical total system design approach to provide more optimum, uniformly reliable, and affordable high-performance structures. It is further hoped that the content of this report may help the specialists to better understand and expand their roles in the total system process, and the novice to appreciate system design analysis.

II. STRUCTURAL SYSTEMS

A shop drawing specifies the component material, it details shapes, sizes, and thicknesses, and it notes interface tolerances and surface finishes; all are structural design related parameters. Requirements for the component may have initiated from an interacting airframe or a machinery system, but the premise of this high-performance structure is the same to sustain a high-probability range of operational environments, optimally, reliably, and at least cost over a specified duration. Between the premise and the shop drawing is a structural system process generating a multitude of performance characteristics, design tasks, interfacing data, multidiscipline interactions, options, trades, and so forth.

The emphasis of this presentation is to demonstrate a process for optimizing system interdiscipline interactions through interface control parameters. The scope is four fold: (1) provide a scheme for identifying and tracking interacting and interfacing discipline tasks; (2) briefly journey through common structural design analyses techniques and processes to characterize input-output interfaces; (3) identify current interface limitations for a reliable and optimally integrated system; (4) interact design tasks with product development tasks for a total system design analysis.

Systems engineering procedures are well documented[1] and are formally enforced in support of project management. A complementary process and format would seem essential for systematically flowing and tracking total system interface tasks in support of design analysis and concurrent engineering. This section sorts common structural characteristics that lead to the development of a structural system interface format. Cost and reliability design constraints imposed on structural systems are offered. Basic statistical and probability techniques used for characterizing observed and derived data are included for convenience. Sensitivity analysis is extensively applied to identify prominent interface design parameters. Structural efficiency analysis is fundamental to high-performance structures and is included. This section summarizes these basics for the understanding and common applications to subsequent sections.

A. Systems Format

Structural requirements and solutions are not only interactive but are also iterative. Where a solution parameter must be approximated in order to proceed with the next design task, a source of iteration is precipitated in which that parameter must be revisited, modified, and interacted as more related information is generated from the evolving design. This behavior of a task, depending on the behavior of other tasks in a set of performing parameters, begs for a system approach to methodically track and resolve the interface interactions and iterations tasks. The structural system process should group root structural characteristics, identify primary and diverging tasks, flow tasks as required to define and optimize interdiscipline performance interfaces, and interact performance design tasks with product development and operational constraints.

Root structural performance characteristics that interface and drive the system are size, shape, environments, materials, integrity, and cost, as listed along the column in figure 2. These characteristics are arbitrarily categorized for their shared scope and along general organizational lines. The initiating root matrix must be small for visibility and manageability, and subtask matrixes are augmented as required.

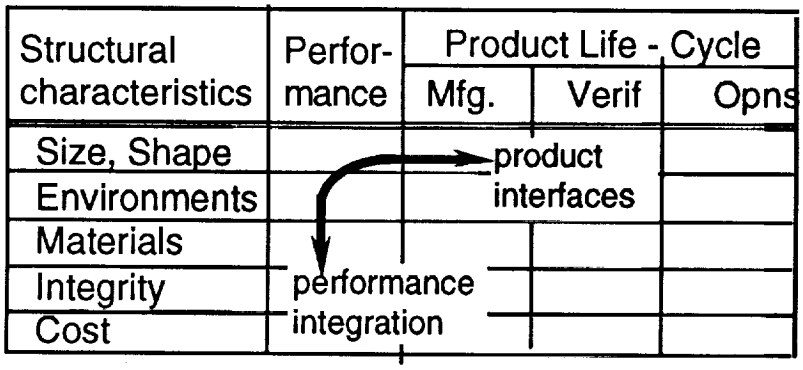

Figure 2. Structural system interface matrix.

These performance characteristics should be listed in the order that they might be completed before the next task may begin. The process usually begins with firm "given" envelope size and operational requirements, and flows through tasks having maximum design maturity, or through those tasks having least consequence on subsequent performance interactions and iterations. Initiating system tasks first estimates envelope shapes and materials from given requirements and integrates them with structural forms. Then they are iterated with updated interface data and dispersions, and finally structural forms are sized to converge on optimum reliable service at least cost.

Performance tasks are further optimized with downstream development tasks and expectations through interaction with manufacturing, verification, and operations interfaces. Tolerances are traded for performance and manufacturing cost. Clearly, the total system design is optimized by synthesizing the ideal structural system interface performance vertically along the performance column, and simultaneously interacting resulting performance design parameters with consequential product life-cycle events horizontally along the rows.

The product life-cycle events are likewise interacted, and methods are optimized along their respective columns with cost and precision and are made customer-friendly along the rows. Customers encompass processors, machinists, welders, assemblers, quality controllers, handlers, operators, etc. Verification tasks include designing the product to facilitate testing for structural performance under operational simulation, and for measuring and monitoring critical design control parameters through development, production, and operational life.

This cross flow of product life-cycle event tasks with structural performance tasks completes the total system matrix proposed in figure 2. Matrix intersections across and along all rows identify sets of interacting tasks. Interfacing tasks topics are accompanied by narratives defining requirements, analyses, deficiencies, and solution options. The format should assist in initiating, tracking, and assuring cohesive life-cycle design analysis, bridging multidiscipline tasks, identifying and optimizing sensitive designer control parameters, accommodating passive parameters, challenging marginal concepts, and bubbling up critical integrating issues. These are the essence of concurrent engineering which this study aimed to support.

B. Balanced System

A necessary condition imposed on a system is accountability, or balance: balance between structural requirements buildup and a common and compelling limiting parameter. That binding parameter is the project least-cost requirement. Least cost of a structural system design may be based on explicit cost, relative costs of similar existing products, or relative cost of solution options. Cost estimates may be translated into another mutually common parameter, weight. Weight is an engineering parameter routinely calculated for performance and tallied for components, assemblies, and systems throughout the system's engineering design phase. Weight may be correlated to size and performance, and it is the most often used parameter to estimate product cost. Cost estimating, tracking, and controlling should be an established, crucial function within concurrent engineering and diligently exercised by integrating structural designers schooled and supported by cost analysts.

Cost per unit weight of a product varies with different types of structures and settings. Complexities directly increase cost. Cost varies inversely with production quantities. Advancing state-of-the-art increases the costs of learning new phenomena, potential bottlenecking, and

allocating new facilities. Cost models must be updated for inflation and technology improvements, and should be adjusted for stretch-out policies.

Payload cost per unit weight is based on the integrated cost. For a given propulsion system, a structural weight reduction of a final-stage structure is an equivalent payload increase and a corresponding decrease in cost per unit weight. Structural weight decrease on a first stage may only increase the payload capability 10 percent, with a corresponding decrease of payload delivery cost. Performance cost trades vary with number of stages and applied technologies along the total system.

Life-cycle costs consider all undertakings that generate costs which include design, development, operations, support, repairs, and reliability. Operational costs are unique to each program and should be estimated from detailed scenarios developed with all interacting systems of figure 1 during the concept phase of systems engineering. The scenario should include flight traffic schedules, facilities, logistics, skills, etc. Structural operational cost analyses should consider structural configuration, expendable versus reusable, and cost of risk to payload owner for lost opportunities from launch delays and flight insurance.

Reliability, like cost, is another system-constraining parameter that is common to all structural disciplines and parts, and is specified to bound and control the integrity of a product. If underdesigned, the product will have a predictably high probability of premature fatigue or overload failure with consequential costs. If arbitrarily overdesigned, it will have an unnecessarily high reliability which increases recurring costs of production, logistics, and nonoptimum delivery performance.

Reliability is traded with cost of ideal performance, operational turnaround time, repair downtime, and all other product life-cycle expenses. It may turn out that moderate reliability margins and high manufacturing cost are traded for low performance and high durability on reusable products. Large margins may be traded for low manufacturing cost and high reliability of expendables. System cost and reliability budgets are controlled through selection of design options using concurrent engineering criteria which include risk assessment. Risk is simplistically defined here as the product of the probability of failure and the cost consequence of failure.

Total system reliability and performance may be designer controlled through interacting design parameters at interdiscipline interfaces. Too often disciplines impetuously accept interface data from preceding disciplines as inputs and then optimize performance within their realms without qualifying their sensitivities and probabilities, nor optimizing their interfaces. It should be recognized that each design discipline serves concurrently as a customer and a supplier. Each receiving discipline should, therefore, work with all interfacing disciplines to obtain quality inputs to achieve optimum performance, and should, in turn, be perceptive and solicitous to its customer's demands for continuously improving interface data quality.

Performance interfacing tasks in the proposed matrix are sources for identifying significant interface control parameters. Geometry is a designer-controlled parameter. Size is designer controlled within manufacturing, logistics, and cost constraints. Dimensional tolerance may be designer controlled for maximum performance, but must be researched and optimized along the row with manufacturing and verification interactions and expectations, and then down the columns with costs.

Natural environments are not designer controlled, except by restricting operations to only moderate conditions which may decrease product cost, but increase recurring operational downtime costs. Materials are designer selected within their structural performance and manufacturing precision and costs. Probability ranges and margins are system and designer controlled. Robust designs favor the selection of low-cost materials and broad property and dimensional tolerances. These and other discipline interface parameters should be identified for performance sensitivities and designer controllability to provide a balanced structural system.

Ultimately, interface analyses should identify uncertainties and define sensitivities and probabilities of all performing disciplines' input-output data. Integrity integrates loads, materials, and stress interface probabilities into a total system that performs well and is dependable. Cost analyses enforce the "how" and "how much" of the system life-cycle services that are affordable.

C. Characterization

Interface data and design parameters are characterized for sensitivities, probabilities, structural efficiencies, and optimizations with system performance, reliability, and manufacturing to minimize the product initial and recurring costs. A summary of basic principles and techniques used in data characterization and design analyses common in subsequent sections follows. It may be reviewed now in preparation for their impending applications, or the remaining section may be deferred until the included principles are referenced.

Variations are inherent in all observed phenomena and are of little information in raw form. Physical data development for structural design is experimentally measured and must be statistically formatted for input to discipline interfaces. The mean "μ" of a set of "x_i" observations describes the central location, or centroid, of data and is defined by the first moment formula,

$$\mu = \frac{1}{n} \sum_{i=1}^{n} x_i \ , \tag{1}$$

for "n" observations. The standard deviation "σ" is a measure of variation from the mean, and it is expressed by the second moment formula,

$$\sigma = \left[\frac{1}{n-1} \sum_{i=1}^{n} \left[x_i - \mu \right]^2 \right]^{\frac{1}{2}} \tag{2}$$

The coefficient of variation,

$$\eta = \frac{\sigma}{\mu} \ , \tag{3}$$

gives the relative variation with several sets of data, and it is a good index of the quality of phenomena. Data with smallest coefficients gather closest to the mean. Typical coefficients of variation of aerostructural material properties are 0.08 or less, structural weights are less than 0.02, and thrust is about 0.015.

Observed data are further characterized by their distribution: normal, lognormal, Weibull, and many others. Unless the sample size and coefficient of variation are large, a normal probability density function,

$$f(x) = \frac{1}{\sigma\sqrt{2\pi}} \exp - \frac{1}{2}\left[\frac{x_i - \mu}{\sigma}\right]^2 , \tag{4}$$

may be assumed. Normal distribution is the most developed theory, it is commonly observed in scientific phenomena, and it is justified by the central limit theorem (CLT). The statistical characterization of normally distributed random variables is completely determined by the mean and standard deviation which makes normal distribution the most expedient and easiest to apply. To assume other distributions for small sample sizes is to prematurely define a trend that is contrary to the CLT, and to unnecessarily impose burdensome statistical information that has not been substantially demonstrated.

Since most environmental data are based on limited sample sizes and simulations, and since most material properties exhibit small coefficients of variation, a normal distribution is a reasonable first choice. Where a phenomenon is known to be non-normal, a split normal is as good a design assumption as most of the other 40 distribution assumptions. Because engineering problems involve only one side of a distribution, the assumed normal mean is defined by the peak frequency point of the distribution, and the standard deviation is calculated from the desired low or high side of the skewed distribution. Innovation and simplicity within the realm of reality is traded over eloquence to increase understanding and to reduce labor intensity and lead time. Normal distributions are considered throughout the text.

There are two specific types of structural statistical data: one is the operational forcing functions that induce stresses on structural forms; the other is material strength of structural forms that resists the induced stresses. Forcing function data are based on limited measured environments, assumed to be normally distributed, and characterized with means and standard deviations. To specify this data input for a specific event such that any required proportion of the data population may be represented in the response analysis, the forcing function interface data may be controlled through the tolerance limit specification,

$$T_L = \mu \pm N\sigma , \tag{5a}$$

or, in using equation (3),

$$T_L = \mu (1 \pm N\eta) . \tag{5b}$$

The designer controlled N-factor specifies the probability proportion (range) as illustrated on the probability density distribution in figure 3. A positive deviation defines the upper tolerance limit assigned to environments, and a negative range factor refers to the lower tolerance limit used by resistive materials. Engineering design data are generally one-sided maximum or minimum.

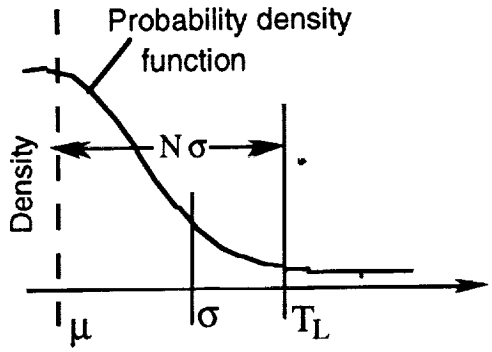

Figure 3. Upper tolerance limit.

The one-sided probability range, specified by N = 1, 2, and 3 standard deviations about the mean of a normal distribution, is calculated to capture 68.3, 95.5, and 99.7 percent of the phenomenon population, respectively. Currently, there is no uniform criterion for specifying forcing function probabilities across projects. Most projects specify a 3-sigma for all forcing functions, while others specify 3-sigma only for high-risk events. Where other types of data are defined by means and extreme tolerances, extreme tolerances are customarily assumed to be 3-standard deviations.

These statistical principles apply to a single variable, but some data observations include multivariables and dispersions from different sensing and measuring instruments on numerous types of dimensions and specimens. Input environments and responses are calculated from a multitude of measured design properties. Two or more mutually exclusive and statistically characterized variables may be combined to define a multivariable function by combining their dispersions through the error propagation laws.[2] When two or more independent variables are added, their standard deviations are "root-sum-squared" (rss) by the summation function rule,

$$\text{for } z = x+y; \quad \sigma_z = \sqrt{\sigma_x^2+\sigma_y^2} \ . \tag{6}$$

When independent variables are multiplied and/or divided, their coefficients of variation are root-sum-squared according to the power function rule:

$$\text{for } \quad z = x^n y^m, \ \eta_z = \sqrt{n^2\eta_x^2+m^2\eta_y^2} \ . \tag{7}$$

Exponents may be negative or positive as they divide or multiply, respectively.

Sample size and standard material acceptance criteria are interrelated and represent a vital data interface control. Tolerance limit is a quality control specification used in determining limits from a probability density plot for a given proportion of data. As an example, 1.96 true standard deviations are required to capture 95 percent of data from equation (4) distribution. However, true values of the mean and the standard deviation are not generally known from small sample sizes, because they may not contain a given portion of the population estimated by equations (1) and (2). In other words, the same test conducted on the same number of specimens by different experimenters will result in different means and standard deviations because of the inherent randomness in the specimens and testing. The population must contain results from all these experiments.

To insure, with a certain percentage of confidence, that the given portion is contained in the population, a K-factor is determined to account for the sample size and proportion. Figure 4 provides K-factors for random variables with 95-percent confidence levels with three commonly used probabilities in one-sided normal distributions.

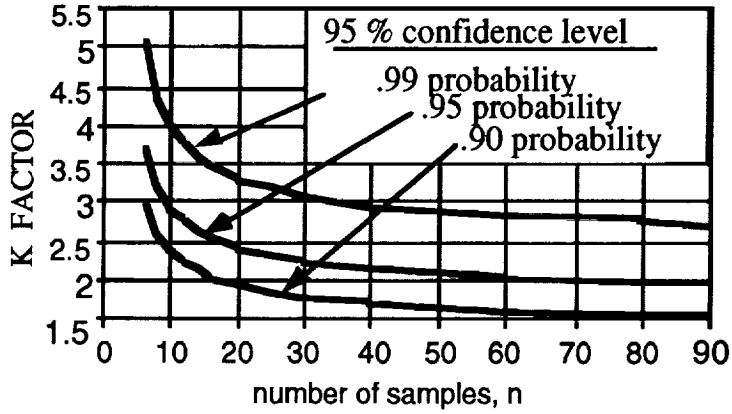

Figure 4. K-factor for normal distribution.

Through the K-factor, a maximum or minimum design value may be determined for a specified probability and confidence. That maximum value for a material property, F_R, is the lower tolerance limit (negative side of fig. 3) representing the weaker side of the material property distribution, and is defined by,

$$F_R = \mu_R - K\sigma_R \,, \tag{8a}$$

and substituting equation (3), yields

$$F_R = \mu_R(1 - K\eta_R) \,. \tag{8b}$$

Note in figure 4 that the designer controlled K-factor rate increases sharply for all probabilities using less than 30 samples. Decreasing the sample size decreases the allowed material performance expressed by equations (8), and it is compounded when the material coefficient of variation in equation (3) is large. If a large coefficient of variation is owed to poor material property control, the trade is expanded to include the life cycle cost of material performance with cost of improving property control, increasing sample size, or both. The cost of standard tests is usually proportional to the selected sample size.

Most of NASA and DOD material properties are specified by "*A*" and "*B*" basis. The "*A*" basis allows that 99 percent of materials produced will exceed the specified value with 95-percent confidence. The "*B*" basis allows 90 percent with the same 95-percent confidence. Figure 5 illustrates a one-sided normal distribution of an A-basis specification having 99-percent probability and 95-percent confidence. The small and large sample size confidence distributions in figure 5 show the reduction of property defined by the K-factors in figure 4 and equations (8). The K-factor is designer controlled by specifying the basis or the specimen size.

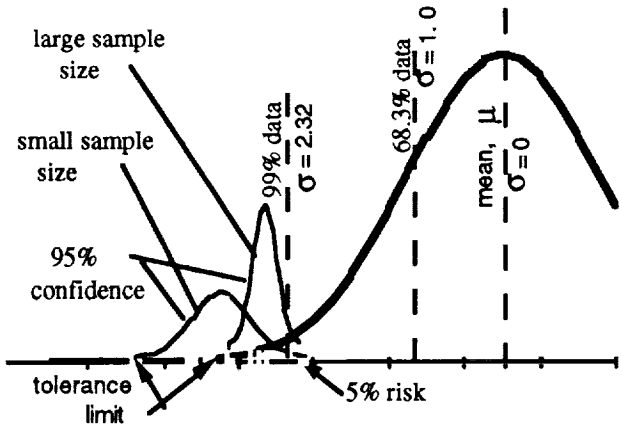

Figure 5. One-sided normal distribution with A-basis.

Properties of common materials are documented in many different sources using different standards. Rarely are they published with the statistical mean and standard deviation parameters that define the A- or B-basis property. These parameters will be seen later to be essential for statistically integrating the material and environment interfaces into a system reliability. Reference 3 provides A- and B-basis properties using a Weibull distribution with results almost identical to using normal distribution in earlier issues, as was expected of small coefficient of variation data. The applied Weibull distribution may be statistically sound, but may be argued as arduous and an engineering overkill.

Reporting statistical parameters of materials should be more beneficial, and perhaps necessary, for current design trends. In the meantime, workable preliminary $K\eta_R$ product may be approximated from referenced properties, and the mean is calculated from the reported deterministic lower tolerance limit property. Design uncertainty margins and accuracies required of these statistical parameters are traded for their sensitivity and consequence to system performance, total reliability, and cost of developing specific data.

Not all design variables are of equal importance to structural performance. To determine their sensitivities in a plant equation (stress, strain, stiffness, weight, cost, etc.) having more than one variable, the partial derivative of each inquired independent variable is calculated and then divided by the plant equation. For example, a plate weight is given by,

$$w = \rho BLt. \tag{9a}$$

Taking the derivative of the weight with respect to thickness,

$$\partial w = \rho BL\partial t\,,$$

and dividing the left side by the left side of equation (9a) and the right side by the right of the same equation,

$$\frac{\partial w}{w} = \frac{\partial t}{t}\,, \tag{9b}$$

results in a directly proportional weight-thickness relationship. The weight sensitivity to bending stress is determined by substituting the allowable stress, F_A, and thickness relationship,

$$t = \left[\frac{6M}{BF_A}\right]^{\frac{1}{2}}, \tag{9c}$$

into equation (10a),

$$w = \rho BL\left[\frac{6M}{BF_A}\right]^{\frac{1}{2}}. \tag{9d}$$

Taking the derivative of weight with respect to stress,

$$\partial w = -\frac{1}{2}\rho BL\left[\frac{6M}{BF_A}\right]^{\frac{1}{2}}\frac{\partial F_A}{F_A}, \tag{9e}$$

and dividing by the weight of equation (9d) as before,

$$\frac{\partial w}{w} = -\frac{1}{2}\frac{\partial F_A}{F_A}, \tag{9f}$$

indicates that increasing the allowable stress decreases the weight at only half that rate. Sensitivity analysis is an essential tool not only for improving performance, but for identifying significant designer control parameters, determining manufacturing tolerance, developing acceptance criteria of raw and stock materials, and establishing verification and quality control standards and inspection points of manufactured products. It is an analytical basis for gaining behavioral perceptions for designing structural efficiency and robust products.

Optimization techniques are extensively applied through all system interface integrations. A candid optimization technique is to partially differentiate a function of more than one variable. It is optimum if the first derivative is zero, and maximum if the second derivative is negative. Lagrange multipliers and steepest-descent methods are commonly used in structural optimization analyses.

These data characterizing and design-optimizing techniques are part of a journeyman's elementary skills. They are the basis for more expediently and completely developing optimum and reliable interfaces, and are extensively applied in decision making and analysis of critical, high-performance structural interfaces. They should be particularly applicable to computerized design data output to gain phenomenon insights otherwise buried in the electronics works.

III. SIZE AND SHAPES

Sizes, shapes, and tolerances are the end products of structural design analysis, which completely describes a component in blueprint. They are the integrating tasks of all discipline output interfaces, and of all manufacturing and operational expectations and constraints. Sensitive interface control parameters are identified, characterized, and optimized with performance, reliability, and cost.

Matrix interface disciplines and interactions are briefly discussed and demonstrated by example. These orderly interactions and flow are in the best nature of a coherent system approach. They raise the physical realities that spark the inquiring process to generate tasks and develop optimum interface solutions systematically and totally.

A. Interfaces and Interactions

Designer-controlled structural sizes and shapes of interest are the envelope shape to accommodate the "given operational environment within a given envelope size," and the material cross-sectional shape (form) and size of selected structural elements constructing the envelope. The shape envelope is optimized with given environments to improve system operational performance by reducing friction, drag, heating, and other induced environments. Then sizes and shapes are interacted with all interfacing structural performance and development disciplines. Ultimately shapes and forms are iterated and optimized with induced environments, materials, reliability, and total costs to establish thicknesses, areas, moments of inertia, and masses. Performance tasks flow horizontally along row interfaces before dropping down the column to the next performance task.

The "given" envelope size and operational environments usually initiate the structural design process by interacting along the matrix row in figure 2 for logistics and facilities constraints foreseen from manufacturing, verification, and operational events. Then size and shape estimates drop down the matrix column to optimize load paths and minimize induced environments. Shapes are interacted with material selection and fabrication methods which include forgings, castings, spinning, welding and so on. They must be compatible with existing manufacturing techniques to provide high yield at least cost,[4] and with large tolerances to reduce rejects and quality inspection points.

Structural element forms are shaped and sized to satisfy local strength and stiffness required to sustain internal loads induced from external operational environments acting on the envelope shape. Interface tasks must also assure that shapes and form sizes are accessible for verification and inspection of critical dimensions, and convenient for recurring assembly, handling, and servicing operations. If shape design parameters are too complex, the product will be difficult to reproduce. If it is hard to assemble, then it will incur assembly errors. The structure must be simple to verify so as to avoid acceptance of defective parts.

Manufacturing environments, such as welding and heat treatments which may distort shapes and sizes, must be resolved in early design phases through controlling parameters, tooling, or circumventing options. Logistics environments on sizes and shapes must be assessed for damage control to minimize expensive repairs and rejects.

Underlying design is robustness. Robustness requires a least-cost method of manufacturing, with low-cost materials, generous tolerances, minimum verification and maintenance requirements, and maximum duration. Identifying sizes and shape tasks, defining respective requirements, developing solution options, selecting design candidates, optimizing interfaces, updating, and iterating complete the structural design cycle within the systems engineering design process.

B. Shape Development

Perhaps an abbreviated and informal design scenario may demonstrate the dynamics of size and shape interactions and optimizations with other interfacing performance and development characteristics. Consider the preliminary design of a pneumatic system that requires a mass of compressible fluid to be filled to a minimum initial pressure p (given environment) and calculated minimum total volume v (size tolerance limit). The internal pressure acts on a container constructed from a candidate material having a density ρ and allowable (upper tolerance limit) stress, F_A. No external environments have been defined at this point.

Starting along the development characteristics row in figure 2, no specific manufacturing and verification constraints on size are noted, but the energy content of pressure and total volume presents an operational hazard. Since the minimum initial pressure is fixed, the volume is split into a number of smaller size containers (v_1) to be clustered into the totally required volume, v. A common size container to satisfy the safe unit energy content is favored by the concept of maximum use of standard parts and minimum cost from manufacturing, verification, and operations expectations. Cost difference for increasing container parts, inventory, and assembly should be accounted.

Shape and size design analysis consists of a series of interface optimizations of integrating disciplines. Intuition based on experience may suggest optimum configurations, but dominating structural shapes must be analytically and thoroughly verified. The preferred membrane shape which minimizes inplane shears on a pressurized container is a symmetrical shell of revolution. It would seem that a shell having maximum volume with minimum surface would result in minimum weight. A cylinder with shaped end-closures whose total surface area is optimized with volume will degenerate into only two hemispherical end closures (maximize volume, minimize area, and solve for the partial of cylindrical length). It can also be shown that a pressurized shell having the meridional curvature approaching the hoop curvature produces minimum and uniform membrane stresses (another optimization analysis).

These optimized design parameters define a spherical membrane whose shape diameter, D_1,. surface area, A_1, and shell form thickness, t_1, are respectively calculated from

$$D_1^3 = \frac{6}{\pi} v_1 , \quad A_1 = \pi D_1^2 , \quad t_1 = \frac{pD_1}{4F_A} . \tag{10a}$$

If all the selected structural performance parameters along the column in figure 2 were optimized, then the shell weight is performance optimum, and the weight is expressed by

$$w_1 = A_1 t_1 \rho = \frac{\pi \rho}{4 F_A} p D_1^3 . \tag{10b}$$

These performance derived shape, form, and size parameters must now be interacted along the matrix row with development parameters to increase yield and reduce costs, which include reduction in unit-to-unit parameter variations (sensitivities) and rejection rates of defective parts (manufacturing complexities).

The two geometric control variables are the shape (spherical) diameter and the form (shell) thickness. Their sensitivities to dimensional variations influence the trades between performance, reliability, manufacturing, and production quality control. Sensitivity of delivered weight with diameter and thickness variations is derived from partial differentiation of the above weight equation (10b),

$$\frac{\partial w}{w_1} = 3\frac{\partial D}{D_1}, \qquad \frac{\partial w}{w_1} = \frac{\partial t}{t_1}. \tag{10c}$$

A 1-percent change in diameter size with the same initial pressure results in a 3-percent change in weight. Thickness tolerance is shown to be a third less sensitive than the envelope size tolerance. Taking partials of the third of equation (10a) will show that stress increases proportional to diameter increase (loose tolerance), which reduces reliability, and stress is only half as sensitive to thickness decrease.

Suppose the low-cost joining method selected was to butt weld the two hemispherical shells. Identical hemispherical shapes represent minimum number of parts, tooling, inventory, maximum use of standard parts, and minimum length of butt weld, all of which are downstream expectations. Minimum weld length decreases the cost of the process. It also increases the reliability of a pressurized vessel, since decreasing the length decreases the probability of incurring an increment of a fateful strength defect in the weld chain.

Though the materiel selected may be compatible with size, shape, form, and operational environments, it must be assessed for manufacturing environments. The weld strength determined from weld coupon tests (verification requirement) is often less than the parent material, and the manufacturing thermal environment of the butt-welding process creates an abrupt mismatch which introduces local shears and moments. Cost of tooling and production labor is then traded with mismatch tolerance to minimize discontinuity stresses and rejection rate. Only a narrow band of thicker shell along the girth weld is analytically required to compensate for the weld strength deficiency and mismatch discontinuity stresses.

Increasing the total shell thickness to the butt weld required thickness is traded to reduce manufacturing and verification development efforts over the band-shell sculptured thickness. The uniformly increased shell thickness will increase total weight, but trading a little performance (within the weight budget) for a more economical manufacturing, verification, and quality-control shape should reduce the net cost of the finished product and packaging. Also, increasing the body thickness should provide a safe margin for abrasive handling of high pressure, notch sensitive bottles. All are downstream interface expectations.

The shape and size must also be compatible with existing facilities, prevailing logistics, and minimum related training and labor for a least-cost life-cycle structure. Gas bottles require operational means for handling, assembling, and supporting them, all of which generate inertial environments at selected supports. Thin plate chairs, or clips, may be shaped and welded onto the bottle surface such as to spread the support interface loads over wide shell areas in tangential shear. Innovative interface shaping should optimize strength before increasing structural thickness and, therefore, weight. The size and number of supports should minimize weight, inventory, handling, and manufacturing costs. Support arrangement should avoid load redundancy to reduce design uncertainties and improve structural support efficiency.

Shape and size options may be iterated further to optimize cluster envelope size and performance. Consider the bottle containing the same fluid mass and shape, but sustaining a higher initial pressure p_2. Applying Boyle's gas law, $pv_1 = p_2 v_2$ = constant, to the volume of equation (10a) yields a new diameter (size) as a function of the new optional pressure,

$$D_2^3 = D_1^3 \frac{p}{p_2} \ . \tag{10d}$$

Substituting this new diameter and pressure relationship into the above shell weight equation (10b) results in no change in optimum performance weight. Because Boyle's law is a constant energy content expression, the option results in no change in operational hazard, either. But a smaller diameter with no change in the system initial and final pressure requirements does result in less gas residual weight which aims to improve delivery performance. It also decreases the weld length and increases the weld thickness with a net increase in weld volume,

$$\Delta v = kD_1^2 p_1 \left[(p_2/p_1)^{\frac{1}{3}} - 1 \right] . \tag{10e}$$

The butt weld mismatch performance and production cost should be reassessed for the increased thickness and weld heat effects.

As more environments are identified and imposed on the structure, more options must be generated, more optimization analyses are required, and more discerning selection criteria must be formulated. Very often, solution shapes accommodating one set of environments introduce new environments that must be integrated, and the envelope must be reshaped to provide optimum performance. Fluid environments may introduce acoustic, thermal, and flutter environments through shaping. Aerodynamic shaping may reduce drag. It may induce a more severe aeroheating environment which may be accommodated with structural and insulating materials selections. Thermal straining of insulating materials must be compatible with the bonded primary structure.

Shapes and forms are designer controlled parameters. The gas bottle example demonstrated the interaction and preliminary optimization of shapes, forms, and sizes with induced environments and product development using nominal dimensions and properties. But all design parameters embody tolerances and dispersions which must be characterized for sensitivity and significance to performance and manufacturing costs. An outline of interfacing design parameters dispersions with performance characteristics leading to manufacturing tolerances follows, and interactions are discussed in subsequent sections.

C. Tolerances

Selecting materials, shapes, and dimensional tolerances involves critical design trades affecting performance reliabilities and manufacturing costs which essentially establish product robustness. Pursuing the gas bottle, with its optimized shapes and developed sensitivities, provides the performance side of the tolerance interface with manufacturing. Optimizing this interface with the manufacturing and production side is unique to each product and requires research for best available techniques relating to lead times, precisions, and costs.

The bottle shape, size, and structural form were optimized for hazard, environments, and performance. The sensitivity of fluid and bottle weights with diameter are identical (equation (10c)). The bottle being heavier than the fluid, the diameter tolerance is traded between performance and cost of manufacturing precision and inspection. Environments are internal pressure and flight forcing functions on supports and duct fittings. Pressure tolerance is based on observed fill and relief valve pressure dispersions per valve and for redundant valves. Forcing function response dispersions are discussed in section IV.

Material selection is founded on the fluid chemical compatibility, manufacturing shaping and joining, and strength features with specified tolerance limits which include dispersions, equation (8a). Materials characteristics and applications are briefly covered in section V. The bottle minimum thickness is determined from the integration of loads, materials, stress, and their dispersions to satisfy deterministic or reliability criteria presented in section VI. Thickness tolerance is traded between performance of equation (10c) and cost of manufacturing and inspection precision.

This brief scenario demonstrated the interactions, trades, and integrations of the total system interface design process. Product design is the integration of all design disciplines input which begins with envelope sizes and shapes, and concludes the cycle with final form sizing and tolerances.

IV. ENVIRONMENTS

Environment characterization, material selection, and design integrity set the framework for developing the ideal structural system performance and reliability. Of the three disciplines, the environmental data, with its variations, duration, applied sequence, and combinations, is the least known during most design phases. Though environment is often the design prime driver, it is also the most difficult to verify and simulate during product development. Consequently, underestimation of operational environments and sneak anomalous combinations are potential service failures. They may be attenuated through applied experience of similarly successful structural systems, large safety margins, or educated understanding of environmental effects and sensitivities on structural systems.

This section characterizes the more commonly imposed aerospace environments, their interface and process with a classical structural response technique, and characterizes and controls limit load output as required for integration with subsequent discipline interfaces. Environments are classified here as degrading, natural, and induced, according to their origin and consequences.

A. Degradation

Life-cycle environments that progressively weaken structures through irreversible changes in material mechanical properties are identified and generally defined in early design phases. A structure may degrade through chemical environments, such as operational interfaces with chemical reagents, or through mechanical environments, such as vacuum, erosion, stress corrosion, wear, and dynamic and thermal fatigue. The structure may also irreparably weaken from downstream manufacturing, assembly, and logistics environments, and from assorted abrasive operations.

Degradation rates are mostly related to material exposure intensity and duration, and an example of a common chemical exposure degradation among metallic structures is corrosion. Metals have a chemical affinity to revert to their original oxide, or earth existing compound, in the presence of such reagents as water, air, acids, halides, and sulfur. The basic rate of corrosion depends on the material's relative position in the electrochemical series. The effect of surface corrosion on strength is to uniformly reduce material cross section, or worse, to localize the corrosion (pitting) that cause surface stress concentration. If the required duration to corrosive exposure is significant, the structure may be thickened, surfaces may be coated, or a less reacting material may be selected.

Vacuum is a mechanical type of hostile environment to a class of spacecraft materials. Carbon-epoxy composites are sometimes used on structural mounts for precision space pointing instruments because of their minimum thermal distortion feature. However, out-gassing properties of some composites cause alignment distortion, which may be prevented by sealing the structural surface. Solar heat also causes structural distortion through direct and unsymmetrical localized exposure, and through poor heat conduction across riveted and bolted joints.

Solution options and selection criteria relating to degrading environments must consider optimum structural performance, operational duration, least cost, state-of-the-art materials, manufacturing techniques, high production yield, least maintenance and spares, damage tolerance and repair, verification and inspection simplicity, and associated skills. Understanding the mechanics of material degradation is necessary for interacting disciplines to identify and resolve hostile environment interfaces.

B. Natural

A class of environments that interfaces externally to structural shapes is the natural environments which include temperature, humidity, pressure, density, winds, and gravity. These are development and performance environments in which the structure operates. Actual values of natural environments cannot be known in specific events, but may be statistically characterized for controlled interface inputs. They act on the structural envelope which induces environments that must be sustained by structural forms. Most natural environments are not designer controllable, but their effect on performance must be understood and minimized through smart material selection and skilled shaping options.

Another class of environments interacting during product development is those experienced in manufacturing and fabrication processes. They may act directly or indirectly to induce variations in structural properties and dimensions ranging from variations in process controls and facility ambients to tolerances and workmanship interfaces. Where controlled processes of critical structural parts are suspected of being unreliable, reshaping should be considered or compensating margins supplemented onto performance solutions.

Verification constraints on environment simulations which may compromise fidelity of test results must be identified in the earliest design phase, and sensitivities and redeeming transfer techniques incorporated into the design analysis. Protoflight test requirements must also be resolved during early structural design phases. Structures that operate in microgravity that can only be verified in an Earth environment would seem to be designed for ideal space performance and compromised for test. These downstream development interface requirements, issues, resolutions, and verification environment trades must be considered through the evolving design.

C. Induced

Natural and in-flight vehicle-induced environments would include aerodynamics, thermal, propulsion, acoustics, shock, inertia, pressure, trajectory controls, etc., which translate into displacements, loads, and moments. Aerodynamic pressure distributions primarily produce aeroheating, center of pressure, drag forces, and vehicle moments. Mass properties establish the center of gravity and moments of inertia. Flight controls induce bending moments and shears, and propulsion induces primary inertial loads.

Because environments are only statistical estimates for specific events, the resulting induced environments and loads should also represent statistical estimates characterized by their mean and standard deviations. Wind speed, shear, frequencies, and gusts bear large statistical dispersions with time and altitude. Thrust and thrust misalignment exhibit dispersions from one unit to another. Propellant loading, sloshing, and residuals vary through flight time and from flight to flight. Speed and acceleration vary throughout the flight. Production articles generally vary in weight and stiffness from unit to unit. Therefore, induced environments generated with probability controlled data input must also provide probability characterized response data. Not all environment dispersions are equally significant to structural performance, and sensitivity analyses should screen the meaningful ones to reduce the number of response cases to be run.

Envelope arrangements and shapes are the most effective design characteristics to minimize the intensity of response loads and moments. Pugh suggests optimizing the structural shape through load line response diagrams using basic theory of structures. Load-line starts and endings must be clearly defined and should be direct and straight. Structures must be arranged to provide the shortest load paths. Divided load paths that are tortuous and leading to ill-defined load must be avoided. Redundancy may improve safety, but it is always inefficient. Inertia is a significant load source on structures and dynamic machinery to be optimized. Increasing strength-weight efficiency lightens the structure, but decreases stiffness and increases dynamic effects. Stub structures decrease dynamics effects. Increasing the structural stiffness at point loads may reduce dynamics environment. These design techniques generate multidiscipline interfaces which should be characterized and optimized.

Design interactions of environmental performance with downstream manufacturing expectations are dimensional tolerances, interface joint rigidity, and margins. Small bolt-to-hole tolerances improve structural stiffness and loads, but increase fabrication and assembly costs. Assembly and handling environments of very large structures are sometimes more severe than operational. Optimum structural designs should simplify flow patterns of induced environments and associated verification requirements. An understanding of environmental excitation effects on elastic structural response follows as a prerequisite for controlling and integrating loads discipline interfaces.

D. Response

Structural internal loads and moments induced by environmental excitations are predicted from mathematical models in modal or matrix form. Models are used to compute response accelerations and forces for determining quasi-static design loads. Modeling approaches and complexities are unique to the services of each structure. Reference 5 discusses the complexities of loads modeling stemming from the diversity of events, the statistical nature of event data, and the necessity of computing sufficient cases and combinations to assure capture of maximum probable

design loads. Stepping briefly through a commonly applied structural dynamics technique should provide the insights for evaluating the probabilistic input-output data process and its compatibility with subsequent interface integrations.

Aerospace loads modeling uses established computational structural dynamics principles and solution techniques[6 7] for multidegrees-of-freedom (MDOF) structures. Current math models assume the structural system to be represented by a network of finite elements designated along the body possessing mass, damping, and stiffness. Natural and induced environments act as forcing functions at discrete grid points. The motion of the total structure is composed of a system of substructures which are expressed by the linear matrix differential equation,

$$[M]\{\ddot{X}(t)\} + [C]\{\dot{X}(t)\} + [K]\{X(t)\} = \{F(t)\} \ . \tag{11}$$

The acceleration matrix, $\{\ddot{X}(t)\}$, is the time dependent physical coordinate at each DOF. The $[M]$, $[C]$, and $[K]$ coefficients are mass, damping, and stiffness matrices, respectively. The forcing function $\{F(t)\}$ is a matrix of time-dependent environmental excitations acting along the structural body. Its matrix rows represent discrete grid points of body internal DOF at which natural or induced environments are acting at one instant of time. Its columns represent time increments. Equation (11) is comprised of a set of coupled equations of motion which may be uncoupled through the mode-superposition method to determine the response of a system to a set of forcing functions.

The system's undamped natural frequencies "ω" and mode shapes $[\phi]$ are solved from the undamped eigenvalue problem, $([K]-\omega^2[M])\ [\phi] = 0$, to obtain the coordinate transformation,

$$\{X\} = [\phi]\{q\} = \sum_{r=1}^{N} \phi_r q_r(t) \ , \tag{12}$$

where q is the generalized coordinates for r = 1, 2, 3, ..., N modes. The shape matrix $[\phi]$ rows represent the mode shape values at each DOF grid point, and the columns represent different mode shapes relating to each natural frequency. Substituting equation (12) into equation (11) and pre-multiplying by the transpose of the mode shape, results in the equation of motion in terms of modal matrices and generalized coordinates. Because of orthogonality, coefficient matrices are diagonal matrices, and the uncoupled system differential equation of motion reduces to

$$[I]\{\ddot{q}(t)\} + [2\zeta\omega]\{\dot{q}(t)\} + [\omega^2]\{q(t)\} = [\phi]^T\{F(t)\} \ , \tag{13}$$

where

$[I] = [\phi]^T[M]\ [\phi]$ is the generalized (unity) mass matrix,

$[2\zeta\omega] = [\phi]^T[C]\ [\phi]$ is the generalized damping matrix,

$[\omega^2] = [\phi]^T[K]\ [\phi]$ is the generalized stiffness matrix,

$[\phi]^T\{F(t)\}$ is the generalized force. (14)

Damping may be assumed to be 1 percent of critical damping, ζ. Typical values for critical damping vary from 1 to 5 percent with lower values assumed at lower frequencies. Given a set of forcing functions, the generalized force is calculated from equation (14), and the generalized coordinates $\ddot{q}, \dot{q}, q$ are then determined by integrating equation (13) for events characterized by associated forcing functions. Substituting these generalized coordinates into equation (12) yields the desired system physical coordinates $\ddot{X}, \dot{X}, X$.

Finally, these physical coordinates are used to compute the substructure internal loads to form a set of quasi-static design loads determined through a loads transformation matrix (LTM) of the inquired internal loads. Applying the substructure's stiffness matrix into the modal displacement method, the internal loads $\{L(t)\}$ of the substructure are given by

$$\{L(t)\} = [\bar{K}]\{\bar{X}(t)\} \ , \tag{15}$$

where $[\bar{K}]$ selects rows of the substructure stiffness matrix corresponding to the desired internal DOF grid points, and

$$\{\bar{X}(t)\} = [T]\{X(t)\} \ , \tag{16}$$

is the total substructure displacements. The $[T]$ matrix selects the substructure DOF out of the system displacements. Equation (15) may be written as

$$\{L(t)\} = [LTM]\{q(t)\} \ , \tag{17}$$

where

$$[LTM] = [K]\ [T]\ [\phi] \tag{18}$$

is the load transformation matrix. The resulting maximum and minimum internal loads, $\{L(t)\}$, are the desired quasi-static design loads.

A similar transformation matrix[8] for substructural global stress analysis may be derived. The displacement matrix of equation (16) is reduced to unit displacement (strain) and then related to stress through material properties relationship and equation (17). The resulting substructure induced stress is computed from

$$\{\sigma\} = [\sigma]\ [LTM]\ \{q(t)\},$$

or

$$\{\sigma\} = [SLTM]\ \{q(t)\}, \tag{19}$$

where $[SLTM]$ is the stress transformation matrix.

Different substructures experience highest internal loads for different environments during different operational events and times. Hence, different substructures are designed by different events and times, and necessitate computation of sufficient loads cases to capture their service maximum load condition over loads histories. The skill, labor, and machine time required in search of maximum response loads increase significantly with increase in (1) structural modeling complexity and interface interactions, (2) number and combinations of forcing functions experienced for each developmental and operational event, and (3) number of significant forcing functions having meaningfully large statistical dispersions.

Structural modeling is a joint effort of stress and loads analysts using finite element methods (FEM) and sharing the basic grid network. Fluid and thermal discipline grid work using FEM or finite difference methods must interface and be compatible with the stress FEM model network. The grid network is selected to accommodate global and detailed local stress analyses. A cylindrical shell would require a circumferential and longitudinal network of grid points as necessary to converge on the global stress state, and a finer grid mesh at structural regions experiencing stress concentrations. Stress concentration regions requiring local complex detailing may be readily identified by abrupt changes in applied loads, geometry, temperatures, and metallurgy.

Mass-spring properties of global models are initiated from preliminary stress analysis of each substructure based on assumed static initial conditions of worst-case events. Because model development is a successive approximation and iteration process, generous sacrificial margins are initially applied to form design parameters to minimize subsequent stiffness and stress design iterations converging on the specified final system reliability.

Usually the loads community utilizes the basic structural model, but reduces the computation time by retaining only those grid points from the stress model that significantly influence the internal load response. Local fine mesh at stress concentration regions is of incidental interest to loads response, but the flexibility of joint connections may be formidable. Stiffness tests of assembled structures have been noted to be softer (as much as 15 percent) than model predictions, which translate into submarginal loads. Part of this discrepancy is shared by the FEM grid modeling, and some is shared by joint modeling. This observation is particularly true for shear pinned or bolted assemblies due to bolt-to-hole and hole-in-line tolerances. Additional flexibility is incurred by bolt-to-hole contact strain and wear which are less present in riveted joints. Flexibility increases with joint use.

Typical joint flexibility models should be analyzed with randomly distributed tolerances and test verified, and design factors should be derived and applied to response analyses. Stiffness modeling must be verified for FEM modeling convergence, and updated with maturing stress and weight progression. Stress is most sensitive to a coarse mesh size. Accuracy converges as the mesh is refined, but rounded errors can become a problem for large systems with too fine a mesh.

Substructural loads and global-stress analyses using the stress transformation matrix of equation (19) with reduced grids should be performed by the loads analyst. This initial, semi-autonomous approach would reduce data transfer and interface coordination across organizational lines, reducing lead time during intense iteration cycles. The detailed stiffness, loads, thermal, and stress modeling and the final comprehensive analyses are the ultimate coordinated responsibilities of the respective disciplines.

Operational events that design structural parts on transportation systems are broad range and are especially so on space launch vehicles. Events that design vehicle substructures include on-pad assembly, lift-off, max Q, high-g, separation, etc. Assembly and logistics environments must also be analyzed for possible maximum design loads. Launch vehicle forcing functions used to generate ascent generalized forces defined by equation (14) include: vibrations and acoustics; wind speed, shear, gust and direction; propulsion thrust rise, oscillations, and mismatch; thrust vector control angle and rate; vehicle acceleration and angle of attack; mass distribution; other trajectory generated environments.

Each of these event categories, criticalities, and combinations constitutes structural response conditions often leading to several hundred loads cases in search of maximum and minimum design loads. Sensitivity analyses should identify events that determine critical design loads, and the significance of environment uncertainty in these events. Pressure, thrust, and inertia are better defined than aerodynamic parameters and winds. An understanding of these criticalities combined with data uncertainties should suggest the computational rigor and techniques that are more compatible with the physical realities and design expedience.

The time dependence and statistical nature of each event further expand the search for extreme design loads which compound the magnitude of response cases to be computed. There are techniques currently considered for selecting and defining response cases that minimize the number of response runs. Fractional factorial design[9] [10] and other orthogonal array techniques have been used to screen large numbers of experiments economically. However, loss of some information in the process and the difficulty of estimating the error may require a thorough assessment with currently trusted codes before general acceptance.

Because input environments to response analysis are time dependent and statistically characterized, the induced loads output is also time dependent and of a statistical nature. The response histories at select grid points are illustrated in figure 6, in which a specific time event may produce a maximum internal load for a DOF at one grid point only. Other time events produce maximum loads at other grid points as shown. Where a maximum internal load response is identified at a grid point, the free-body diagram of the included substructure experiencing that maximum response is constructed with all time-consistent loads acting along the total system.

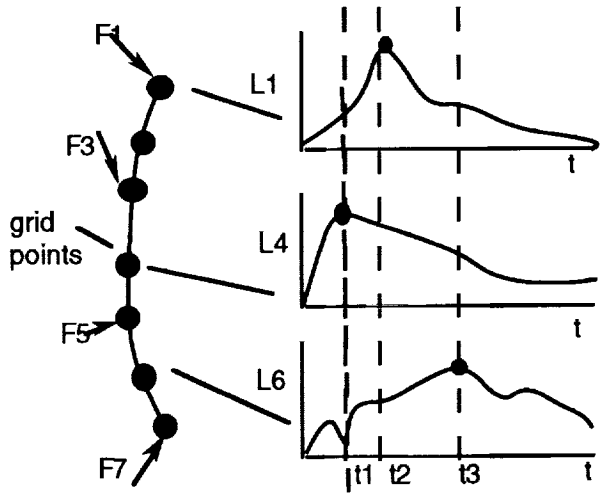

Figure 6. Time-dependent response.

This computational process for designing different parts through time-consistent and statistically dispersed loads is repeated for each substructure at each unique event time producing the maximum load response. The end product of the structural response to environmental excitations is a set of maximum design loads, or "limit loads," and event times for all the system substructures and critical regions. Common practice is to provide response limit loads in deterministic form. The interface problem is to decompose the deterministic limit load into its probabilistic parameters.

E. Limit Loads

Prime interest in the structural dynamics model was to understand its input and output interfaces and the process for implementing quality control between interfacing disciplines. As impressed earlier, environments are derived from observation and, as an interface input, should be characterized by statistical parameters. Therefore, the deterministic limit load output also contains statistical properties which should be decomposed for integrating into the system total reliability.

There are validated techniques and codes currently used to compute load response which accepts and processes statistically specified environments.[11] But most commonly used codes accept probability controlled excitation dispersions, and process them directly into worse-on-worse deterministic output whose statistical characteristics are undefined and cannot be integrated with interfacing disciplines as required by equation (6). Furthermore, response load probabilities along the total structure should be adjustable through the control range factors "*N*" in interfacing with applied stress and strength disciplines to produce a specified uniformly reliable system.

It is recognized that current deterministic response estimates are expedient, direct, adequate, and even desirable during iterative design cycles, and no new technology or disruptive process should be imposed or suggested. However, it would seem reasonable to require post-final response computations to provide the statistical parameters of the limit load output. This underlying requirement leads to probing through the classical structural dynamics analysis outlined above to evaluate the worse-on-worse response deviation, and to characterize the statistical parameters controlling interface probability.

The above structural dynamics response method was used with provision for specifying all forcing functions inputs in tolerance limit format. The MDOF configuration was modeled similar to figure 6 with time-dependent forcing functions at every grid point. Numerical values were assigned to springs and masses, but time-dependent forcing functions were entered symbolically as F_i into the dynamic equation (11), which included initial conditions. It was processed through equation (17) with the response load of the grid point "*g*" substructure maximized with event and excitation times. The result was expressed with symbolic forcing functions and "c_i" response gains,

$$Lg = c_1(F_1)+c_2(F_2)+c_3(F_3)+c_4(F_4)+c_5(F_5)+ \ldots\ldots, \tag{20}$$

influencing the respective grid point. The resulting equation (20) defines a linear combination of the elements of a random vector[12] having a combined mean,

$$\mu_g = \sum_{i=1}^{n} c_i \mu_i , \tag{21}$$

and a combined variance of

$$\sigma_g^2 = \sum_{i=1}^{n} (c_i \sigma_i)^2 . \tag{22}$$

The resulting combined standard deviation,

$$\sigma_g = \left[\sum_{i=1}^{n} (c_i \sigma_i)^2 \right]^{\frac{1}{2}}, \tag{23}$$

is also an extension of the summation function rule of equation (6).

Symbolic forcing functions F_i are statistically derived and characterized through the upper tolerance limit format of equation (5b),

$$F_i = c_i \ (\mu_i + N_i \ \sigma_i). \tag{24}$$

Since the structural dynamic analysis is linear, all symbolic forcing functions may be converted into their tolerance limit at any point in the response analysis. Applying equation (24) into the response of equation (20) yields the response load with uniquely specified probability ranges,

$$Lg = c_1(\mu_1 + N_1 \sigma_1) + c_2(\mu_2 + N_2 \sigma_2) + c_3(\mu_3 + N_3 \sigma_3) + \ldots \ . \tag{25}$$

Collecting terms from equation (25) reduces the load response to the sum of the combined mean and the combined variation terms,

$$L_g = \sum_{i=1}^{n} c_i \mu_i + \sum_{i=1}^{n} c_i N_i \sigma_i \ . \tag{26}$$

While the first term on the right side of equation (26) is identical to the combined mean of equation (21), the second term reflects the worse-on-worse input-output process and does not conform to the appropriate root-sum-squared output rule of equations (23) and (6). Their statistical qualification was one objective of this dynamic analysis. The other objective was to access and modify the probability response terms required by equations (21) and (23), to properly define the load tolerance limit output,

$$L_g = \mu_g + N_g \sigma_g \ . \tag{27}$$

Substituting equations (21) and (23) into equation (27),

$$L_g = \sum_{i=1}^{n} c_i \mu_i + \left[\sum_{i=1}^{n} \left[c_i N_i \sigma_i \right]^2 \right]^{\frac{1}{2}}, \tag{28}$$

expresses the necessary load response tolerance limit in combination with elements of the random vector. Having tracked the forcing function from input through output, and exposing its response gains, terms, and deficiencies, it was possible to demonstrate the construction of expression of equation (28) from a worse-on-worse response routine to satisfy the tolerance limit required by equation (27) through a sample problem.

First, the load response of a current computational method was simulated using worse-on-worse tolerance limit forcing functions in equation (25), and a deterministic (single constant) response load output "L_g" was calculated as currently practiced. Then substituting only nominal forcing function μ_i inputs (without dispersions) into the same program that produced equation (25), the nominal load response was computed,

$$\hat{L}_g = \sum_{i=1}^{n} c_i \mu_i \,. \tag{29}$$

Subtracting this nominal response of equation (29) from the deterministic response calculated from equation (25) and squaring gave the appropriate variance response of equation (22) combined with the range factor. This is the same expression as the second term squared in equations (27) and (28),

$$\left[L_g - \hat{L}_g\right]^2 = \sum_{i=1}^{n} \left[c_i N_i \sigma_i\right]^2 = N_g^2 \sigma_g^2 \,, \tag{30}$$

which is the proper response probability range. The next step required a subroutine to calculate the combined response variance of each forcing function (random vector) as defined by equation (22). Dividing the response variance of equation (22) into the response probability range of equation (30), produced the third and final statistical property which is the response probability range factor squared:

$$N_g^2 = \frac{\left[L_g - \hat{L}_g\right]^2}{\sum_{i=1}^{n} \left[c_i \sigma_i\right]^2} \,. \tag{31}$$

However, only the results of equations (25), (29), (30), and (22), are required to construct the desired interface tolerance limit control. The probability range factor is designer adjusted for specific systems, and the range factor N_g of equation (31) was derived here only to further assess the worst-on-worst output.

Applying the $N_i = 2$ probability range factor to all forcing functions resulted in a 10-percent higher N_g factor response. Because the combined rss standard deviation was less than the combined worse-on-worse deviation, the response N_g was expected to be larger in order to satisfy equations (26) and (28). The analysis was repeated with $N_i = 3$ giving approximately the same higher percent response. Their consistent percent response may be related to the consistent set of gains and forcing functions used in all cases.

However, in applying different input N_i-factors to different forcing functions, the combined N_g-factor response was dominated by those forcing functions associated with the largest "c_i" response gains. None of the output response range factors were less than the lowest input N_i-factors, nor were they necessarily as high as the highest input. Varying the distribution of N_i-factors over the response c_i gains seemed to significantly vary the limit load L_g of equation (25). Fractional factorial schemes for estimating the sensitivities of input parameters and maximizing the response load given

in equation (25) may be an expeditious approach. Symbolic modeling used in this analysis is limited by the DOF size. Specifying a common range factor N to all forcing function input may simplify the computation.

This exercise was too restricted to project or confirm more definitive trends, but it did demonstrate that combined output probabilities should and could be determined through a combined response and decomposition analysis within existing codes, and without interrupting design iteration cycles. More importantly, it revealed that response $N_g\sigma_g$ probabilities are not necessarily expected to be the same as input probabilities $N_i\sigma_i$. Thus, it follows that all substructural response loads should not be expected to be uniformly reliable within the structural system which argues for output interface controls.

Combining computational results of equations (29) and the square root of equation (22) into the tolerance limit format of equation (24), the interface output load is controlled by:

$$L_{gc} = \hat{L}_g + N_g\sigma_g \ , \tag{32}$$

where N_g is the designer control range factor that may be specified by the loads discipline. Ultimately, loads and thermal environments interact with other interfacing disciplines to establish the applied stress response expressed by:

$$F_A = \mu_A(1+N_A\eta_A), \tag{33}$$

where the range factor N_A is adjusted for the integrity analysis, section VI.

Aeroheating environments experienced through ascent trajectories determine the convection heating rates which are computed into structural temperatures. Temperature environments interface with structural and insulating materials and with stress disciplines to select materials and calculate form dimensions. Though thermal environments represent a major structural design discipline, they were not developed and interacted here both for brevity and because they represent the same class of boundary value solutions as the dynamics and inertial loads demonstrated using similar interface and control approaches.

V. STRUCTURAL MATERIALS

Structural materials are the resistive matter to structural environments. Their numerous mechanical properties establish and respond to all structural discipline interactions sequentially and in combinations such that structural materials cannot be treated alone. If environments were noted to be the structural system drivers, materials are the reputed hub of all the structural system performance and manufacturing interactions. Because of materials' multiproperties interactions, it is important that interfacing disciplines understand the structural relationships of material properties, in general, and their behavior, sensitivities, and limits with interfacing environments, mechanics, reliability, and manufacturing in detail.

Through that understanding and collective insights, structural materials analyses and applications may be improved, new applications discovered, and interface integration enhanced.

Understanding the response and limits of property interfaces is simplified by classifying the multitude of commonly used structural materials by their basic load-displacement analog, by the response and limit with each type environment, and by their sensitivities with structural forms.

The three basic material mechanical analogs are elasticity, plasticity, and viscosity. Their mathematical expressions are unique to their content of unit force (stress, σ), unit displacement (strain, ε), and time or rate dependency. These models are further combined to define mechanical behavior of more complicated engineering materials as noted in figure 7.

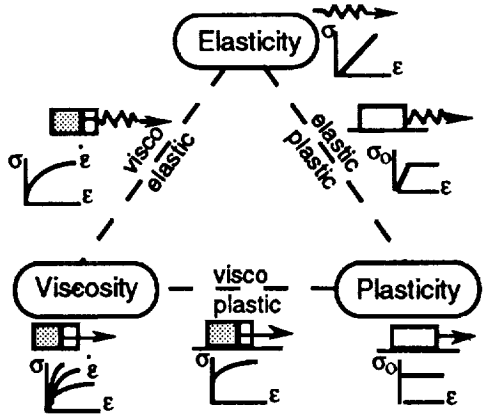

Figure 7. Material analogs.

A mechanical spring conceptualizes an elastic material which is defined by a linear relationship of stress and strain through a proportionality constant. Elasticity[13] is the most developed mathematical theory of the three analogs and is the most applicable to high specific strength materials. For these practical reasons, elastic material behavior with induced environments and structural forms is the best understood and modeled, and the general mechanical behavior and design approaches are often cloned into other materials.

Elasticity theory is a boundary value problem as are fluids, dynamics, heat transfer, acoustics, and other mechanics problems using piecewise or pointwise solutions. A classical plane stress elastic problem consists of integrating the compatibility equation,

$$\frac{\partial^4 \phi}{\partial x^4} + 2\frac{\partial^4 \phi}{\partial x^2 \partial y^2} + \frac{\partial^4 \phi}{\partial y^4} = 0 \ ,$$

and satisfying the loads and displacement boundary conditions through the constants of integration. The stress function, Φ, is defined by the three components,

$$\sigma_x = \frac{\partial^2 \phi}{\partial y^2} \ , \ \sigma_y = \frac{\partial^2 \phi}{\partial y^2} \ , \ \sigma_{xy} = \frac{\partial^2 \phi}{\partial x \partial y} \ ,$$

derived from equilibrium. Thermal elastic radial displacement may be modeled in cylindrical coordinates and in the plane strain condition by satisfying the appropriate stress function and the compatibility and equilibrium equations,

$$\frac{d^2u}{dr^2} + \frac{1}{r}\frac{du}{dr} - \frac{u}{r^2} = \alpha\frac{(1+\nu)}{(1-\nu)}\frac{dT}{dr}.$$

The fourth condition in elastic theory is the boundaries which are satisfied through the constants of two integrations. Elasticity theory solves many problems (especially local stress patterns) exactly, but it is limited to physical models that can be solely expressed by stress functions. Strength of materials theory circumvents stress functions by selecting simple slim and thin structural elements (long beams, shells, plates, long columns, torsion rods, etc.) with specific boundaries and equilibrium conditions. It solves most problems remote from boundaries exactly. It is the most versatile and commonly applied analytical technique. FEM's and the boundary element method (BEM) are the most universally used computational methods.

Ideal plasticity[14] is analogous to a sliding friction block in which a material will strain only after reaching its unique plastic stress "σ_0" level, and will continue to strain at that constant stress in a constant strain energy flow. There are many applications for plastic models in processing and manufacturing, in stress concentration and failure modes, and in combination with other structural analogs. The plastic-elastic behavior of polycrystalline materials stressed beyond the elastic limit is a real material property of applied interest.

Viscosity (or Newtonian) models do not necessarily represent structural materials, but the concept incorporates the time dependence in real materials as in viscoplastic processes and visco-elastic ancillary structures. Viscoplasticity is used to model Bingham materials such as wet paint and solid propellant mixing properties. The material will strain at rates proportional to stress rates after exceeding the plastic stress of that material. It is useful to estimate interacting environments and loads it imposes on mixers and conveyor structural systems.

The spring-dashpot series and parallel concepts of viscoelasticity are applied to polymer-based materials exhibiting time-dependent behavior as in constant strain-rate, creep, and relaxation conditions. Vibration isolators, gaskets, seals, flexible membranes, and inflatable structures are common applications. Viscoelastic materials used in rocket systems have a wide range of properties, durations, and degradation modes. Some have not been successfully characterized for bonding to steel cases as liners, insulation matrices, and solid rocket motor propellants. Though these applications are not selected for their structural attributes, their capacity for induced flexing and thermal straining must be compatible with that experienced through their bond on primary structures. Viscoelasticity is an evolving theory, and most current developments are documented in rheology journals and subject technical papers.

A. Metallic Properties

Of the three basic analogs in figure 7, elasticity and plasticity represent the generic behavior of most real structural materials, and auspiciously, both are embodied in metallic primary structures. Specific material interface properties of interest are those related to thermal, density, stiffness, displacement, and strength and to their limits. For shortness of presentation, only polycrystalline materials and their pivotal interface properties and sensitivities to performance and product development interactions are explored. Interface behavior insights reaped from these metallic properties may be modified and analytical approaches projected onto similar materials.

The single most common observation of polycrystalline behavior is the applied stress and the measured strain response. Uniaxial tension tests are the simplest type for obtaining the most commonly used mechanical properties of structural materials. Figure 8 typifies the stress-strain relationship of a polycrystalline material achieved from such a test. The segment O–σ_o is the linear elastic region of the material which is governed by the resilience between atoms within a crystal. When an applied load is relieved, the deformation will recover to its original position, "0". Plastic flow is the permanent deformation caused by the displacement of atoms to new crystal lattice sites. The ratio of elastic stress and plastic flow defines the inelastic slope, and their change rate characterizes the nonlinear property of the material beyond the elastic limit, σ_o, up to the ultimate stress, F_{tu}.

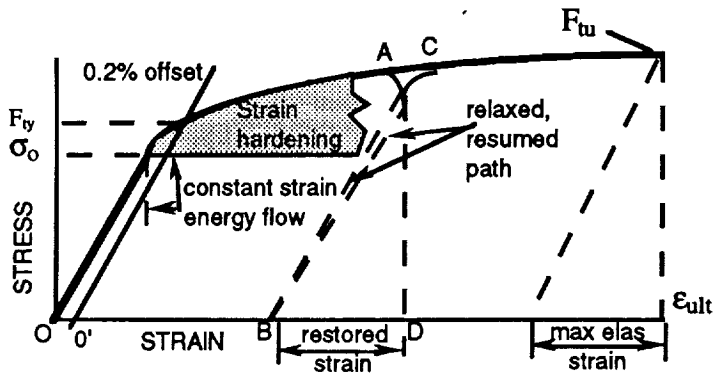

Figure 8. Uniaxial tensile properties of polycrystalline materials.

Many structural design properties required for integrating multidiscipline interfaces are derived from uniaxial tension tests, which include elastic and plastic constants, constitutive equations, and limits. Approximately 90 percent of launch vehicle structural weight is composed of 4130, 4140, and D6AC steels, and 2024-T81, 2219-T87, and 7075-T6 aluminums. The succeeding properties discussions are confined to the most general applications of aerostructural metallics.

B. Elastic Properties

Most structural systems are designed to sustain operational environments within the linear (elastic) region of the stress-strain curve. The source of this elastic response to imposed environments resides in the microstructure of polycrystalline space lattices. Tetragonal space lattice structures include tin and manganese. Zinc and magnesium form hexagonal shaped lattices, and the cubic space lattice is common for most other metals. The body-center-cubic (bcc) has an atom at each corner and one in the center and is associated with iron, columbium, chromium, molybdenum, and tungsten. Face-center-cubic (fcc) has an atom at each corner and face center and includes aluminum, copper, lead, nickel, and silver.

The space lattice elastic concept may be modeled by springs representing the energy interaction between atoms (fig. 9). The edge springs between corner atoms feature a common spring constant K_1, and all diagonal springs feature another spring constant K_2, for a total of two constants required to define the elastic behavior of a metallic material microstructure.

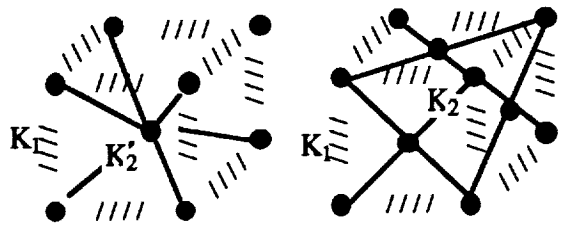

Figure 9. bcc and fcc space lattice structures.

This concept may be extended to assume homogeneous, isotropic, elastic, macrostructure solids in which Hooke's law expresses the extensional elastic behavior as

$$\sigma = E\varepsilon . \tag{34}$$

The proportionality constant E is the Young's modulus which represents the elastic constant K_1 and is defined by the slope of the elastic stress-strain profile in figure 8. Because spacing between atoms changes proportionally with applied load, the space lattice volume also changes. In a uniaxial tensile test, the specimen lateral dimensions contract as the longitudinal load extends its X-dimension. The resulting three dimensional strains are $\varepsilon_y = \varepsilon_z = -\nu\varepsilon_x$, and using equation (34), the Poisson's ratio is defined by

$$\nu = -\frac{\varepsilon_y}{\varepsilon_x} = -\frac{\varepsilon_y E}{\sigma_x} . \tag{35}$$

The constant "ν" is the Poisson's ratio, and it represents the second elastic constant K_2. Elastic, isotropic Poisson's ratios range between 0.26 and 0.33.

Related elastic constants responding to other type loadings may be derived from the above two constants, such as the shear and bulk moduli,

$$G = \frac{E}{2(1+\nu)} \quad \text{and} \quad K = \frac{E}{3(1-2\nu)} , \tag{36}$$

respectively. Where materials do not conform to equation (36) properties, the materials may have been worked to anisotropic conditions, and the Poisson's ratios must be adjusted. It is interesting that these elastic and other mechanical constants (density, specific heat, coefficient of thermal expansion) are insensitive to lattice defects. Limits, such as yield and ultimate stresses, are affected by lattice defects and by temperature which excites the atomic activity. Face-center-cubic lattice materials are more ductile. Alloyed metals form intermolecules which increase hardness and strength.

The three-dimensional stress-strain relationships are derived by superposition of equations (34) and (35),

$$\varepsilon_x = \frac{1}{E}\left[\sigma_x - \nu(\sigma_y + \sigma_z)\right] ,$$

$$\varepsilon_y = \frac{1}{E}\left[\sigma_y - \nu(\sigma_x + \sigma_z)\right],$$

$$\varepsilon_z = \frac{1}{E}\left[\sigma_z - \nu(\sigma_x + \sigma_y)\right], \tag{37a}$$

or

$$\sigma_x = \frac{E\left[(1-\nu)\varepsilon_x + \nu(\varepsilon_y + \varepsilon_z)\right]}{(1+\nu)(1-2\nu)},$$

$$\sigma_y = \frac{E\left[(1-\nu)\varepsilon_y + \nu(\varepsilon_x + \varepsilon_z)\right]}{(1+\nu)(1-2\nu)}, \tag{37b}$$

$$\sigma_z = \frac{E\left[(1-\nu)\varepsilon_z + \nu(\varepsilon_x + \varepsilon_y)\right]}{(1+\nu)(1-2\nu)},$$

and summation is

$$\varepsilon_x + \varepsilon_y + \varepsilon_z = \frac{1-2\nu}{E}(\sigma_x + \sigma_y + \sigma_z). \tag{37c}$$

Since normal stresses do not cause shear strains, the uncoupled shear stress-strain relationships are defined with the first equation (36) shear property,

$$\tau_{xy} = G\gamma_{xy}, \quad \tau_{xz} = G\gamma_{xz}, \quad \tau_{yz} = G\gamma_{yz}. \tag{38}$$

Another derived elastic property is the strain energy per unit volume of the material, and it is defined by the area under the linear stress-strain slope in figure 8,

$$U_o = \frac{1}{2}\sigma_x\varepsilon_x = \frac{1}{2}\varepsilon_x^2 E. \tag{39}$$

Applying the same reasoning to pure shear strain gives:

$$U_o = \frac{1}{2}\tau_{xy}\gamma_{xy} = \frac{1}{2}\gamma_{xy}^2 G. \tag{40}$$

The range of elastic strain is called resilience and is a measure of the material to resist permanent structural distortion. It is especially useful in such mechanisms as springs, bellows, and various flexible joints. The material resilience increases as the yield point increases and the modulus decreases.

Fracture toughness is a material property from which a crack length may be determined to propagate at a given stress level. It is a measure of energy transfer from an elastic stress field of the cracked structure to the process of crack extension. The relationship of local stress near a crack to the half-crack length "*a*" is the stress intensity factor

$$K_{IC} = \sigma\sqrt{\pi a} \quad . \tag{41}$$

The intensity factor K_{IC} on the left side of the equation is a material property, as are any of the above properties, and is independent of crack length, loading system, or geometry. The subscript "*IC*" refers to the most severe crack opening mode having tensile stress applied normal to the crack face in plane strain conditions (thick specimen). Equation (41) denotes the trade inherent in the selection of materials and structural performance. Material selection fixes the intensity factor, and the allowable crack length determines the maximum design stress level. Because high performance structures utilize high specific strength materials, the allowable crack size would be small, but the combination should be selected within inspection detection techniques.

Other design considerations for intensity factors are the strong dependence on temperature, heat treatment, texture, and impurities. The intensity factor varies with size and crack distribution on brittle materials. Strength increases as size decreases, such as in piano wire, because of the reduced probability of finding large cracks in small sections. There is less probability of brittle fracture in stress concentration regions because the high stress acts over a small volume of material which can admit only small flaws, but elsewhere, the lower stress acts over a larger volume allowing larger flaws. The weakest-link concept of brittle fracture is that strength is not determined by the average distribution of flaws, but by the single most perilous flaw. Reference 16 provides a substantive list of fracture mechanics literature.

Over 80 percent of metallic failures are said to result from mechanical environments imposed on limited dynamic properties of materials such as damping capacity, endurance, and impact resistance. Materials will vibrate until the internal friction is dissipated as heat and sound energies. The dissipation energy per unit volume is the damping capacity obtained from a material hysteresis loop for one cycle. The damping capacity is the ratio of the hysteresis energy and the work of deformation. Damping capacity decreases as strength increases. Aluminum and certain heat treatable alloy steels have little damping capacity.

Fatigue stress is repeated stress which slips and breaks atomic bonds in the weakest sites and cluster boundaries, causing microscopic cracks. As the operating stress is cycled, the crack forms a stress concentration which spreads away from the surface until the undamaged core material is sufficiently reduced to snap. The dull appearance on a fatigue fractured surface is caused by the rubbing of cracked surfaces. Fatigue failure usually occurs at stress concentration points so that surface notches naturally reduce endurance. Notch sources are machining, corrosion, inclusions, gas cavities, and violent quenching. The endurance of rolled surfaces is 30 percent less than polished finishes. Some high-strength steels have no endurance limit advantages. Environments, material property variations, manufacturing variations, and many other variations and design considerations affecting endurance are abundantly documented.[17]

In designing for fatigue, the maximum and minimum fluctuating stresses are expressed by the alternating stress parameter,

$$\sigma_a = \frac{1}{2}(\sigma_{\max} - \sigma_{\min}) \, , \tag{42}$$

and the stress ratio,

$$R = \frac{\sigma_{\min}}{\sigma_{\max}} \quad . \tag{43}$$

The relationship of the stress fracture level "S" and number of cycles "N" for any maximum stress and stress ratio are obtained from published[3] S-N curves plotted on log scales for $N>10^5$ cycles. The slope of the S-N curves decreases with increasing cycles, and for many metals, the slope nearly flattens. Stresses below the nearly flat slopes are assumed to endure an infinite number of cycles and are noted as fatigue limits.

The total life cycle of a structure in a dynamic environment may be estimated by the linear cumulative damage rule. The cumulative damage is approximated by the sum of the fractions of life used by each stress cycle,

$$\frac{n_1}{N_1}+\frac{n_2}{N_2}+\frac{n_3}{N_3}+....+\frac{n_k}{N_k}=1\,, \tag{44}$$

where n_i and N_i are the number of cycles used and the endurance cycles, respectively, at the same stress level. The sequence of stress level per life cycle ratio may reduce the cumulative damage rule. Earlier cycles of high stress levels are more damaging to succeeding, lower stress level accumulations, and are compensated by an arbitrary design factor of 4 lifetimes. Hard start machinery and flexible ducts on first-stage gimbaled engines are examples of earlier, high level stress cycles.

C. Elastic Limit

The limit of these elastic properties is reached when atoms displace along cleavage planes and plastic flow occurs within atomic bonds. Plastic deformation starts in different locations, numbers, and intensities, and it is difficult to detect and determine where and how much deformation progressed until large enough parts have been affected. This phenomenon explains why different gauge lengths in uniaxial tensile tests provide different elastic limits, why yield coefficients of variations are higher than strength variations, and why in brittle materials it is more difficult to detect the limit. Hence, an arbitrarily selected standard for defining the yield point of a metallic material is shown in figure 8. The intersection of a line parallel to and offset by 0.2 percent from the elastic slope establishes the yield point, F_{ty}, which is the accepted design elastic limit of uniaxial stress.

The elastic limit of the multiaxial stress state is empirically related to the uniaxial tensile yielding, and it is reasonably consistent with experimental observations. The yield criterion is based on the minimum strain energy distortion theory which supposes that hydrostatic strain (change in volume) does not cause yielding, but changing shape (shear) does cause permanent deformation which is generally related to the uniaxial tensile elastic limit. The multidimensional limit stress criterion is expressed by:

$$\sigma_o=\left[\sigma_x^2+\sigma_y^2+\sigma_z^2-\sigma_x\sigma_y-\sigma_x\sigma_z-\sigma_y\sigma_z+3(\tau_{xy}^2+\tau_{xz}^2+\tau_{yz}^2)\right]^{\frac{1}{2}}\,, \tag{45}$$

and assumes $\sigma_o = F_{ty}$ for yield limit. This criterion is also applicable for relating multidimensional stresses to uniaxial stress at any level of stress. The companion multidimensional strain limit is:

$$\varepsilon_o = \frac{\sqrt{2}}{3}\left[(\varepsilon_1-\varepsilon_2)^2+(\varepsilon_1-\varepsilon_3)^2+(\varepsilon_2-\varepsilon_3)^2\right]^{\frac{1}{2}} . \tag{46}$$

The shear yield stress may be derived from the uniaxial tension test through equation (45) by assuming all stresses are zero except one shear stress,

$$F_{sy} = \frac{\sigma_o}{\sqrt{3}} = \frac{F_{ty}}{\sqrt{3}} . \tag{47}$$

Specific properties and limits vary with metallurgical processing, manufacturing treatment, etc. Exceeding the elastic limit will cause the material to flow at constant strain energy which defines the perfectly plastic solid behavior.

D. Plastic Properties

The stress-strain curve beyond the elastic limit illustrated in figure 8 traces the ductile region of polycrystalline materials. When loaded to point "*A*" and relaxed, the strain decreases elastically to point "*B*". The material will have restored the elastic strain *B*-*D*, and will have permanently deformed with a plastic strain of *O'*-*B*. Upon reloading, the unit load traces a hysteresis loop as it approaches point "*C*" near point "*A*" from which it was unloaded, and then resumes the stress-strain relationship as had it not relaxed.

This plastic flow property of metals from the inelastic limit to ultimate stress, F_{tu}, is responsible for their economic importance in manufacturing processes as in rolling, forging, drawing, extruding, stamping, bending, riveting, and spinning. The manufacturing quality and plasticity properties are leading considerations in trades and in material selection for least-cost production shaping. Another commonly engaging feature in highly sculptured structures is the local plastic transformation and stress redistribution in critically strained regions. This inelastic phenomenon allows the material to flow and redistribute the peak stress optimally and permanently, and then retain the full elastic strength for repeated cycles. This forgiving feature of polycrystalline materials warrants some understanding of inelastic properties.

Modeling plastic behavior could be very difficult unless idealized into the simplest mathematical expressions within the physical phenomena of the material and its application. Where plastic behavior is induced into designs, strains experienced by many common ductile materials are relatively small, which allow engineering stresses and strains to be used with negligible errors. Since strain hardening is a directional slippage process introducing anisotropic properties, design loads on flight structures are limited to increasing inelastically, monotonically, and unintentionally. The elastic limit exceedence is monitored and assessed for reuse. This limitation or assumption simplifies the nominal performance analysis and permits use of available uniaxial tension test data.

There are approaches and techniques for modeling and applying metallic inelastic properties to classical strength of materials elements. Some FEM codes tabulate the nonlinear material coordinates of figure 8 and compute the linear strength of materials behavior with the inelastic property in a piece-wise-linear technique. One analytical approach is to model the inelastic uniaxial stress-strain relationship of figure 8 by the two parameter power expression,

$$\sigma = K\varepsilon^{n}, \tag{48}$$

where "n" is the strain-hardening exponent ranging between 0.10 and 0.40, and "K" is the strength coefficient. The exponent $n = 0$ defines a perfectly plastic solid, and $n = 1.0$ degenerates into Hooke's law of elastic materials. Dislocation is the separation of the slipped and unslipped regions of a crystal, and strain hardening is due to dislocation interactions and pileups. Cold-working increases strain hardening, which increases the exponent n, and is more effective on cubic lattice materials. Cold-working also produces anisotropic properties in which milled structures are expected to sustain a larger strain hardening exponent "n" than the adjacent weld joint material. It should be noted that when the yield points of the base metal and the butt weld filler are significantly different, a metallurgical discontinuity[18] occurs at the bond surface only after the weld filler exceeds the elastic limit.

Perfectly plastic materials are assumed to be incompressible. Using equation (35) to calculate the volume of a plastically stressed specimen in uniaxial tension, and equating it to zero volume change, implies the ideal plastic Poisson's ratio is:

$$\nu_p = \frac{1}{2}. \tag{49}$$

An anisotropic inelastic Poisson's ratio, between yield and ultimate stresses, may be related to the secant modulus defined by the uniaxial stress-strain model of equation (48). The inelastic Poisson's ratio is approximated by:

$$\nu = \nu_p - \left(\nu_p - \nu_e\right)\frac{\sigma}{E}\left[\frac{K}{\sigma}\right]^{n}, \tag{50}$$

where subscripts "p" and "e" refer to the plastic and elastic Poisson's ratios, respectively.

Combined inelastic normal stress or strain behavior is exceedingly complex and requires simplification for understanding and modeling. There are many approximate forms of plastic constitutive equations, and the following are applicable with assumed equation (50) Poisson's ratios,

$$\begin{aligned}
\varepsilon_1 &= \left(\frac{\sigma_1}{K}\right)^{\frac{1}{n}}\left[1 - \frac{1}{\nu\sigma_1}(\sigma_2+\sigma_3)\right], \\
\varepsilon_2 &= \left(\frac{\sigma_1}{K}\right)^{\frac{1}{n}}\left[\frac{\sigma_2}{\sigma_1} - \frac{1}{\nu}\left(\frac{\sigma_3}{\sigma_1}+1\right)\right], \\
\varepsilon_3 &= \left(\frac{\sigma_1}{K}\right)^{\frac{1}{n}}\left[\frac{\sigma_3}{\sigma_1} - \frac{1}{\nu}\left(\frac{\sigma_2}{\sigma_1}+1\right)\right].
\end{aligned} \tag{51}$$

The σ_1 is the uniaxial property of equation (48). The plastic shear stress-strain relationship is similarly approximated using equation (47),

$$\tau = C\gamma^n . \tag{52}$$

The ultimate uniaxial tensile stress F_{tu} is the stress at fracture. For very ductile materials, it is defined as that stable stress point where the strain-hardening that increases stress beyond the elastic limit equals the stress of the decreasing cross section that weakens the specimen. The associated ultimate strain ε_{tu} is obtained from figure 8. Strain hardening property and coefficient are calculated from:

$$n = \log(F_{tu}/F_{ty})/\log(\varepsilon_{tu}/\varepsilon_{ty}), \quad K = F_{ty}/[F_{ty}/E]^n, \quad C = (K/\sqrt{3})[\sqrt{3}/(2+2\nu)]^n .$$

The minimum distortion energy criteria of equations (45) and (46) may be extended to the ultimate multiaxial stress since the material flow continues at nearly constant strain energy from yield to stable ultimate stresses. There are many similarly treated inelastic metallurgical properties as elastic properties which the reader may wish to pursue through the publications of J. Lubliner, T. Miyoshi, J. Necas, W. Johnson, P. Mellor, A. Mendelson, and J. Haddow. Properties and relationships presented above are usually available during design phases, and others may be suitably estimated for preliminary structural design.

It must be recalled that in designing shapes that must be manufactured by exceeding the elastic limit, the subsequent operating strain is reduced by the plastic flow absorbed in the shaping process. Unless the product is annealed, that reduced strain establishes the permanent maximum available for its service life. The maximum elastic strain of a shaped component is the ratio of ultimate stress and elastic modulus,

$$\varepsilon_{e_{\max}} = \frac{F_{tu}}{E} , \tag{53}$$

and having reached less than that theoretical level, the material behaves elastically to that strain, or less, on repeated cycles until fatigued.

This limitation also applies to stress discontinuity regions. A concentrated load or abrupt geometric shape on a structure produces a local multiaxial stress distribution with the highest stresses occurring near the discontinuity. Common examples are holes, bolted joints, key ways, fillets, notches, etc. As the discontinuity stress increases beyond the elastic limit, the strain rate increases faster than the applied stress rate (fig. 8), which allows the nonuniformly increasing stress to spread and be shared by the adjacent less stressed area. The ratio of the increasing applied stress rate and response plastic strain rate determines the local flow stability. The ultimate stress is defined by $F_{tu} = \sigma_o$ in equation (45). Inplane bolt-hole loading and other contact stresses are familiar cases of self-limiting stress concentration.

Inelastic bending stress may illustrate a technique synthesizing nonlinear material models expressed in above exponential form with linear strength of materials models. The method simplifies the algebra and allows continuous integration for more descriptive results. Figure 10(a) is the strain diagram along the beam cross section in which planes remain plane after bending.

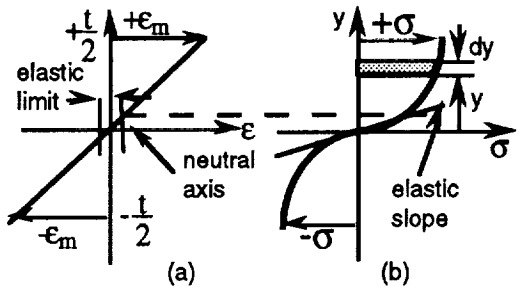

Figure 10. Inelastic bending stress and strain.

The maximum strain at the extreme fibers caused by the moment "*M*" is derived as

$$\varepsilon_m = \pm\left[\frac{2(n+2)M}{Kt^2}\right]^{\frac{1}{n}},$$

and the stress distribution in figure 10(b) is defined by:

$$\sigma = \frac{(n+2)My^n}{2(t/2)^{n+2}}.$$

Note that the stress profile is proportional to the power expression of equation (48), and the slope error at the origin between the elastic and equation (10b) is negligible. The beam shear stress distribution along the cross section is

$$\tau_{xy} = \frac{V(n+2)\left[(t/2)^{n+1} - y^{n+1}\right]}{2(n+1)(t/2)^{n+2}}.$$

Deflections, slopes, and other element inelastic behaviors may be similarly derived analytically using strength of materials theory, or applying FEM codes (notably ABAQUS).

Plate bending stress and strain formulations are complicated by the plane strain condition which engages multiaxial stress relationships of equations (51). A dilemma arises in having to estimate the orthotropic Poisson's ratios which range between the elastic equation (35) and the inelastic equation (50) values. This problem is only as difficult as the accuracy required. A sensitivity analysis will show that the stress related to the plane strain is linearly and inversely proportional to the related Poisson's ratio. Since the bending stress varies along the plate thickness illustrated by figure 10, Poisson's ratio also varies. This Poisson's ratio distribution coupled with the sensitivity about the other perpendicular axis suggests a maximum or average value based on local stresses that is a practical preliminary design way out.

The complexity of combining the nonlinear normal axial and bending stresses is best represented by the orthographic projections in figure 11. Inelastic bending planes again remain plane in figure 11(b), and the key is locating the bending neutral axis from the section centroid through the stress equilibrium of bending tension and compression in figure 11(c). Figure 11(a) is the symmetrical uniaxial stress-strain diagram. It must be remembered that once this combined stress

is applied beyond the elastic limit and released, repeating the combined stress will result in a linear elastic strain relationship up to the maximum stress previously experienced.

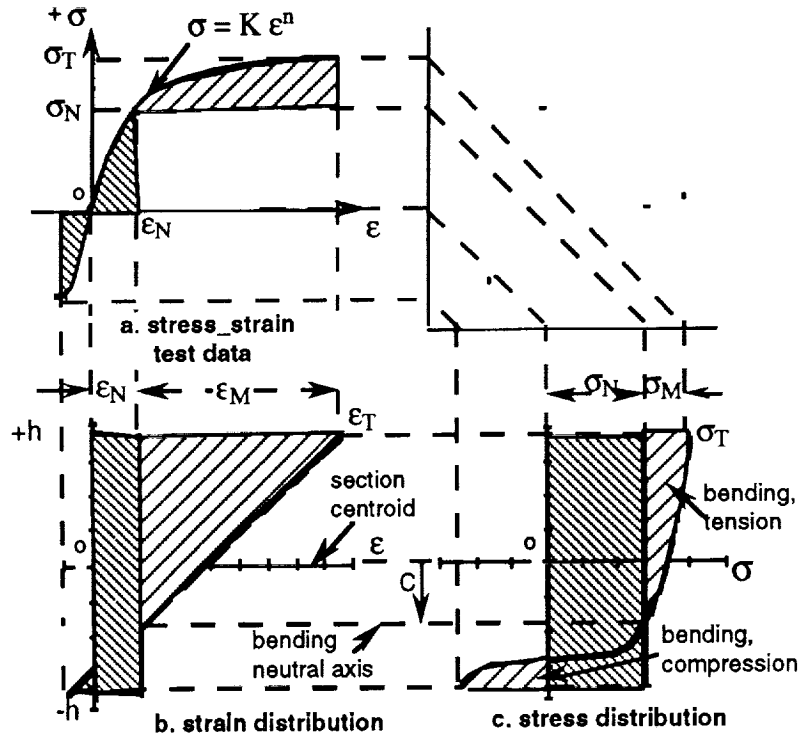

Figure 11. Combined normal tension and bending diagram.

Since the strain history of a test article is often not known, and since strain gauges are the primary sensors applicable in stress concentrated regions, all manufacturing and verification test data uncertainties must be considered in design phases. It should also be recognized that tracking strain gauges alone beyond the elastic range may lead to premature failure for lack of the total residual strain history. This is not unusual when testing previously deformed structures having partially consumed plastic strain.

A common test assumption is that pure normal strain may be separated from the combined strains by averaging back-to-back strain gauge data. Beyond the elastic limit, this formula is shown not to be valid. Though the normal strain in figure 11 is 20 percent of the total strain, it is 60 percent of the total stress. This type loading is not unusual in primary shell structures and pressure vessels, but it should be avoided around butt welds. Plate or shell bending causes the welded joint material with the lowest elastic limit to hinge and assume a disproportionate share of the local displacement. With the combination of lowest elastic limit and bending of the narrow weld width, the weld filler is the first to yield and progressively strain the most to fracture.

A design property of some interest for comparing different materials is the net inelastic stress share of the total strength. Figure 12 shows that aerostructural steels generally have greater strength (clear bars) than aluminums, but also contain more inelastic stress (F_{tu}–F_{ty}) than aluminum. Their large maximum strains qualify as ductile materials. The higher strength steel is three times the density of aluminum, giving neither a specific strength (F_{tu}/ρ) advantage in tension.

The net inelastic stress contribution (darkest bar) to the performance of structures usually occurs in very small but critical regions which would seem to justify the unique data, skills, verification, and development required for designing primary structures beyond the elastic limit. Inelastic analyses are necessarily conducted on stress concentration zones, unexplained failures, stretching performance, and other unique studies supported with inelastic data and computational codes.

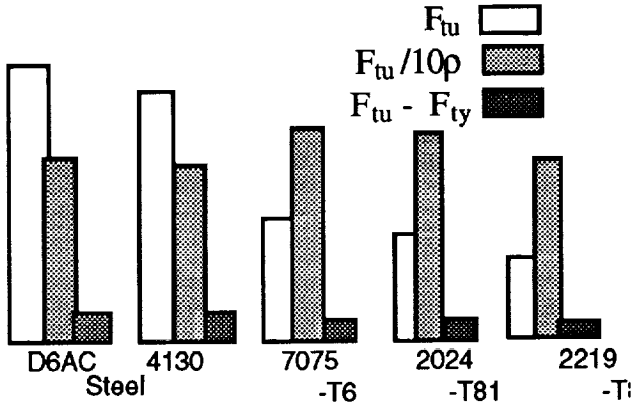

Figure 12. Inelastic performance.

E. Design Sensitivities

With the exceptions already discussed, designing within the elastic limit of a polycrystalline material is a universally accepted practice for the many pragmatic reasons of linear modeling, superposition, physical simile, data availability, etc. Though the material data base of property limits is generally provided and applied with a high standard of reliability and confidence, elastic constants are not as uniquely defined, nor is it practical to treat them statistically in most design analyses. It should be instructive to assess the effects of elastic constant variations on a few common structural elements.

Underlying a structure's design goodness is its reliability and affordability. Affordability is correlated to weight. The analytical technique used was to determine the sensitivity of applied stress interfaces with the elastic constants, recognizing that a deviation in stress is a deviation in reliability. Deviations in structural stiffness matrix applied to equation (1) introduce dynamic loads deviations which also translate into stress and reliability deviations. A deviation in a material constant that exceeds allowable stress must be compensated by increasing form size to reduce the stress and, therefore, increase the weight. This technique highlights the sensitivity of modulus and Poisson's ratio on stress, buckling, stiffness, and weight, using one- and two-dimensional stress elements. Sensitivity formulas are derived for the most general applications.

One-dimensional stress elements are representative of stringers, frames, and rods. Simplifying features of this class of elements are: reliability and weight are not dependent on Poisson's ratio; buckling and axial or bending stiffness may be expressed by the cross sectional area "*A*", elastic modulus "*E*", and coefficients "*C*":

$$P_{cr} = C_p AE\,,\ \mathrm{K} = C_K AE\,. \tag{53a}$$

Coefficients C_p and C_K are functions of loads, radius of gyration, length, and boundary conditions. Using equation (53a) and the sensitivity analysis technique outlined in equation (9), the buckling and stiffness sensitivities to modulus are, respectively,

$$\frac{\partial P_{cr}}{P_{cr}} = \frac{\partial E}{E}, \quad \frac{\partial K}{K} = \frac{\partial E}{E}. \tag{53b}$$

In one-dimensional stress elements, a reduction in modulus results in a proportional reduction in structural stability and stiffness, and a corresponding reduction in reliability. Substituting the areas of equation (53a) into the weight formula,

$$w = \rho A L, \tag{53c}$$

gives the weight sensitivity to the modulus,

$$\frac{\partial w}{w} = -\frac{\partial E}{E}. \tag{53d}$$

Though increasing the material modulus is shown to decrease the structural weight, the sensitivity analysis also suggests that an underestimated modulus would require an increase in the plate sizing which increases the weight proportionately.

Two-dimensional stress elements are exemplified by plate panels, thin shells, and membranes. They are all dependent on modulus and Poisson's ratio. Using equations (37), it can be shown that all steel and aluminum plate reliability parameters of stress, buckling, and stiffness bear the same sensitivity relationships with the modulus in equation (53b) because their Poisson's ratios are about equal. It then follows that the weight penalties are identical to the sensitivity expressed by equation (53d). Sensitivities of reliability and weight parameters to Poisson's ratio are contingent on each plate stress state, loading conditions, and orientation.

Plane stress condition of figure 13 assumes that the stress acting normal to the surface is insignificant compared to inplane stresses.

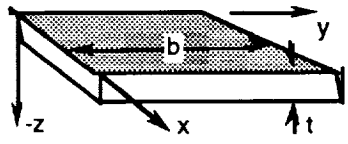

Figure 13. Plate coordinates.

Substituting the plane stress condition, $\sigma_z = 0$, into the last of equation (37b), the corresponding strain from equation (37a) is reduced to

$$\varepsilon_z = -\frac{\nu(\varepsilon_x + \varepsilon_y)}{(1-\nu)}, \tag{54a}$$

and the maximum stress and strain are

$$\sigma_x = \frac{E}{(1-\nu^2)}(\varepsilon_x + \nu\,\varepsilon_y)\,, \quad \varepsilon_x = \frac{1}{E}(\sigma_x - \nu\sigma_y)\,. \tag{54b}$$

The sensitivities of stress and stiffness to Poisson's ratio are:

$$\frac{\partial\sigma_x}{\sigma_x} = \frac{2\nu^2\varepsilon_x + \nu(1+\nu^2)\,\varepsilon_y}{(1-\nu^2)(\varepsilon_x + \nu\,\varepsilon_y)}\frac{\partial\nu}{\nu}\,, \quad \frac{\partial K}{K} = -\frac{\nu\sigma_x}{(\sigma_x - \nu\sigma_y)}\frac{\partial\nu}{\nu}\,. \tag{54c}$$

Using first and second of equation (37b) for the special case of a $\sigma_x = 2\sigma_y$,

$$\varepsilon_x = \frac{(2-\nu)}{(1-2\nu)}\varepsilon_y\,, \tag{54d}$$

and substituting into equation (54c), gives the sensitivities to Poisson's ratio,

$$\frac{\partial\sigma_x}{\sigma_x} = \frac{\nu(1+2\nu)}{2(1-\nu^2)}\frac{\partial\nu}{\nu}\,, \quad \frac{\partial K}{K} = -\frac{\nu}{(2-\nu)}\frac{\partial\nu}{\nu}\,. \tag{54e}$$

Assuming $\nu = 0.33$,

$$\frac{\partial\sigma_x}{\sigma_x} = 0.3\frac{\partial\nu}{\nu}\,, \quad \frac{\partial K}{K} = -0.5\frac{\partial\nu}{\nu}\,. \tag{54f}$$

Plane strain condition assumes $\varepsilon_y = 0$, which is typical of thick plates in bending. Substituting into equation (37a), solving for the corresponding stress, and proceeding as before, the stress and stiffness sensitivities to Poisson's ratio for bending stress only are

$$\frac{\partial\sigma_x}{\sigma_x} = \frac{3\nu^2}{(1-2\nu)(1-\nu)}\frac{\partial\nu}{\nu}\,, \quad \frac{\partial K}{K} = -\frac{2\nu^2}{(1-\nu^2)}\frac{\partial\nu}{\nu}\,, \tag{55a}$$

and

$$\frac{\partial\sigma_x}{\sigma_x} = 1.43\frac{\partial\nu}{\nu}\,, \quad \frac{\partial K}{K} = -0.24\frac{\partial\nu}{\nu}\,. \tag{55b}$$

Critical buckling of a plate may be expressed by:

$$P_{cr} = \frac{E}{1-\nu^2}C_p A\,, \tag{56a}$$

resulting in the stress and weight sensitivities to Poisson's ratio,

$$\frac{\partial P_{cr}}{P_{cr}} = \frac{2\nu^2}{(1-\nu^2)}\frac{\partial \nu}{\nu}, \quad \frac{\partial w}{w} = -\frac{\nu^2}{(1-\nu^2)}\frac{\partial \nu}{\nu}, \tag{56b}$$

or,

$$\frac{\partial P_{cr}}{P_{cr}} = 0.24\frac{\partial \nu}{\nu}, \quad \frac{\partial w}{w} = -0.12\frac{\partial \nu}{\nu}. \tag{56c}$$

It may be generally concluded from equations (54) through (56) results that the reliability properties of stress, stiffness, and stability are proportional to the elastic modulus, and that an underestimated modulus is a reduction in reliability or cost.

To compensate for this uncertainty, an estimate of the accuracy of the test-derived modulus should be useful. Estimating the coefficients of variation of a stress testing machine's 0.3-percent tolerance, specimen dimensional tolerance of 0.3 percent, and strain gauge accuracy of 3 to 5 percent, and applying these variations to the power function rule of equation (7), resulted into a 3-sigma deviation of about 5 percent, with the strain gauge tolerance swaying the accuracy.

Poisson's ratio seems to be less sensitive to plate buckling and stiffness than the modulus, but it is the most significant elastic constant in plane strain and plate bending. Referring to the first of equation (55b), a 5-percent error in Poisson's ratio will produce about 7-percent error in bending stress of a plate. Since Poisson's ratio is the more difficult property to experimentally derive, at least a 7-percent uncertainty in plate bending and fracture mechanics should be considered. Similar sensitivity analyses may be conducted on other mechanical properties affecting structural design, such as density, heat transfer, thermal expansion, and specific heat.

Sensitivity analysis may be used to compare a property of one material with another. Assuming a common buckling load on an aluminum and a steel plate, the thicknesses required of the different plates are calculated from equation (56a). Since the area is related to thickness and the Poisson's ratios and critical loads are equal, the thickness formula reduces to:

$$t = \frac{c_1}{\sqrt{E}}, \tag{56d}$$

and substituting into the weight equation gives:

$$w = c_2\frac{\rho}{\sqrt{E}}. \tag{56e}$$

Dividing the aluminum plate weight by the steel,

$$w_{al} = w_{st}\frac{\rho_{al}}{\rho_{st}}\sqrt{\frac{E_{st}}{E_{al}}}, \tag{56f}$$

gives aluminum about a 40-percent weight advantage. Calculating the weight sensitivity in equation (56f), first with density and then with modulus, reveals that weight is many times more sensitive to

density than it is to modulus. Since equation (56f) is independent of Poisson's ratio, it is applicable to plates, shells, and stringers in buckling and in axial and bending stiffness.

These property comparisons and sensitivities are essential for trading materials with structural forms. Uncertainties and sensitivities in modeling material properties and configuration dimensioning must be estimated and integrated into a reliable and affordable system to establish the structural integrity.

VI. INTEGRITY

The primary purpose of a structure is to sustain operational environments with no detrimental deformation over a specified duration, and to achieve it all at least cost. This integrating and balancing criterion is the measure of structural goodness, of structural integrity. Never has such a bedrock demand been fraught with so much misunderstanding or misuse, and for so long. Digressing momentarily into a brief historical note may accentuate the want of structural integrity in past practices and the importance to insure it on impending ones.

The Saturn first stage intertank shell was constructed with an innovative ring-frame and corrugated skin design. It was a primary load carrying structure, designed to a 1.4 factor of safety, and weighed several tons. Four tail fins were designed on that same stage for control contingency only. They were designed to the same 1.4 factor, aircraft construction, and had a combined weight comparable to the intertank. The intertank failed the structural test well below the required safety factor, and the fins failed at a safety factor of 6.0. The intertank cost a redesign and reverification, the fins cost less Moon-gravel return. Both failed the integrity criteria. Though these types of failures are rare compared to other discipline failures, their failure rate has not improved over decades. The most frequently cited causes in failure investigations are inappropriate assumptions and incomplete analysis.

This section examines and integrates all discipline outputs that define complete structural integrity. Loads, stress, material design probabilities and NASA factor of safety criteria are integrated to establish system reliability. Weight is minimized which correlates to least recurring delivery cost. A structural failure concept is presented with reliability and deterministic techniques for reducing the probability of failure. System uncertainties as sources of premature verification failures are estimated and integrated into deterministic and reliability concepts. The deterministic concept is combined with a first order reliability concept into a deterministic reliability concept to provide a verifiable total system reliability concept.

A. Reliability Concepts

Failure occurs when the applied stress on a structure exceeds the resistive stress of the structural material. This simple concept integrates the statistical interfaces of the measured uniaxial material resistive properties with the design applied probable stresses resulting from measured and assumed environmental data. Applied stresses are multiaxial induced stresses converted into uniaxial stresses through equation (45) to be compatible with the resistive stress interface. The probability nature of these interfaces is completely defined by normal probabilistic density distributions illustrated in figure 14. Their tail overlap suggests the probability that a weak resistive material will encounter an excessively applied stress to cause failure.

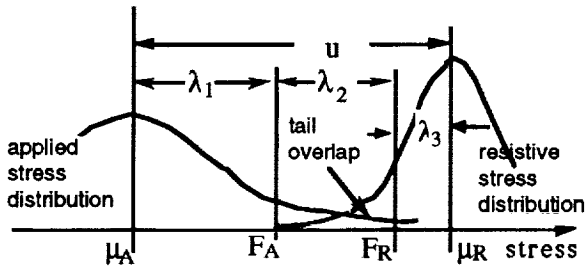

Figure 14. Structural reliability concepts.

The probability of failure is reduced as their tail overlap is decreased by increasing the difference of the resistive and applied stress means, $\mu_R - \mu_A$. Subscripts A and B refer to applied and resistive parameters, respectively. The symbol "σ" refers to standard deviation in this section, and stress is noted by "F".

While there should be no misunderstanding in this failure concept, the difficulty and diversity of results arise from the different techniques used to decrease the interference of distribution tails. There are many techniques investigated[20] and evolving for determining and providing reliable structures, but two that are more compatible with the dynamics of current system design analyses and with the culture of analysts are the first-order reliability and the conventional deterministic methods. Both methods reduce tail overlap with different benefits and limitations.

The first-order reliability method assumes that applied and resistive stress probability density functions are normal and independent, and may be combined to form a third normal expression,[12]

$$Z = \frac{\mu_R - \mu_A}{\sqrt{\sigma_R^2 + \sigma_A^2}} , \tag{57}$$

known as the safety index. The relationship between the safety index Z and reliability R is given by

$$R = P(F_R - F_A > 0) = \phi(Z) ,$$

where $\phi(z)$ is the standard cumulative distribution, and F_R and F_A are the minimum resistive and the maximum applied stresses, respectively. Figure 15 plots this reliability and safety index relationship.

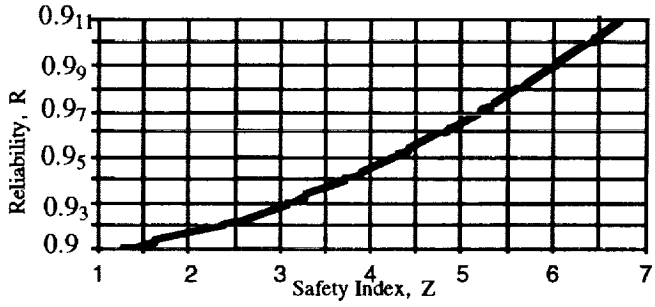

Figure 15. Reliability versus safety index.

The merits of the reliability method are evident from equation (57). Increasing the safety index by increasing the difference of the resistive and applied stress distribution means decreases their tail overlap (as illustrated in fig. 14) and, therefore, decreases the probability of failure. The safety index is seen to be dependent on the difference of the means and not on selected materials strength. In other words, a constant difference of the means defined by the safety index, and by figure 14, may slide up and down the stress axis with no change in tail interference. The safety index is a system concept in that all of the system probability characteristics and disciplines interfacing within the difference of the means are integrated and uniquely quantified.

The difference of the mean is essentially normalized by the combined standard deviation of the two distributions. The greater the distribution dispersions, the greater the distribution difference must be to yield the same tail overlap, implying that loads and applied stress probability ranges should not be selected independent of combined dispersions. Though equation (57) does not allow for modeling uncertainties, they may be estimated and added to the combined standard deviation according to the error propagation laws of equations (6) and (7).

The general implementation of reliability methods on structural design has not been totally probed. An understood requirement on high-risk, quasi-static primary structures is that they must be timely and economically verified. Another concern is the lack of experience and confidence in specifying reliability to different failure modes and to risk analysis.

Rotary machinery failures are normally contained and not necessarily catastrophically threatening. Their loads are usually well defined, operating within the material elastic limit, and failures are almost always fatigue. They cannot be verified to some deterministic safety factor method anyway, because dynamic systems that induce the structural body (inertial) load environments required for verification are not designed to operate much above nominal range. Reliability methods would seem most appropriate for duration failure modes, and reliability selection criteria might be derived from a wide range of commercial experiences.

On the other hand, applying reliability methods on semistatic, primary structures subject to overload failure modes raises philosophical issues. Specifying a reliability to a moderate-cost, high-production product provides the basis for evaluating the cost-of-failure rate consequences over the life cycle of the total high-production output. Specifying absolute reliabilities to very high-cost, low-production rate aerospace carriers and one-of-a-kind payloads provides the failure probability for decision and risk analysis of the carrier and payload, but a generally acceptable reliability criteria for aerostructures has not been developed.

Current practices of specifying safety on ultimate stress on polycrystalline materials would require the difference of the distribution means to straddle the material inelastic region shown in figure 16. The applied stress F_A must avoid operating over the inelastic zone to inhibit the primary structure from permanently deforming and perilously altering boundaries and performance. In so increasing the difference of the applied and ultimate stress distribution means $(\mu_{tu}-\mu_A)$, the tail overlap area decreases, and the safety index increases, which is supposed to increase the reliability according to figure 15. However, as the difference of the means increases, the distribution tail lengths theoretically increase, but the real data content in long thin tails becomes more scarce and the concept and results become more suspect.[21]

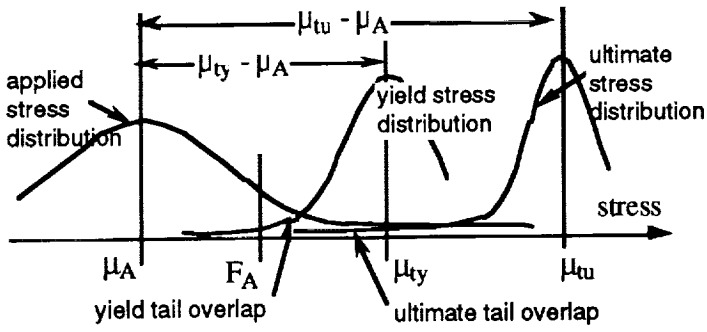

Figure 16. Reliability concept including yield stress.

Applying reliability methods on the yield failure mode as the resistive material property is a viable option because it does increase the data content of the shorter distribution tails, but the method does not currently allow for timely and economical verification on primary structures subjected to overload fracture.

Conventional deterministic method also governs the structural reliability related to the tail interference through the difference of the resistive and applied stress distribution means. In dividing the difference of the means into three distinct zones,

$$\mu = \lambda_1 + \lambda_2 + \lambda_3 , \tag{58}$$

as illustrated in figure 14, the deterministic method bounds and defines only the midzone autonomously and arbitrarily into a safety factor and ignores the probability contributions of the end zones.

Zone λ_1 is the probability range of the applied stress. It is determined from response multi-axial limit loads combined into a Von Mises stress. The range of this zone is currently controlled by the loads community through the specified loads probabilities of the input data, and it is independent of total system safety. The subsequent stress output is provided as a deterministic maximum expected applied stress F_A. Zone λ_3 is the probability range of the resistive stress defined by the *A*- or *B*-basis material selection. It is experimentally derived and documented as a deterministic minimum ultimate strength, F_R. Zone λ_2 is the midzone controlling the applied stress by the conventional safety factor, *SF*,

$$\lambda_2 = (SF-1)\, F_A \ . \tag{59}$$

Until recently, the loads safety factor had been documented[22] as a multiplying factor applied to the limit load to obtain the ultimate load, and it was used to account for uncertainties that could not be analyzed in a rational manner. The conventional safety factor had been and still is based on the limit and ultimate loads. It is expressed in stress terms by

$$SF \times F_A = F_R . \tag{60}$$

Equation (60) interfaces all three zones and governs the tail interference, but not through the combined three zones to define the system absolute probability of failure. The safety factor is

verifiable in that the experimental response stress may be correlated to a multiple factor of the predicted applied stress to fracture as given by equation (60). Imposed experimental test environments inducing the applied stresses are model predicted design conditions. Actual operating environments can only be verified in a limited number of all-up field or flight tests. Combined estimated modeling uncertainties of material, fabrication, and stress are verified from their lumped test response as to exceeding or reducing the specified safety factor.

A weakness in the method is that while a universal safety factor may be imposed on all structural materials, the net safety is dependent on the strength of selected materials which compromises high strength materials. Substituting equation (60) into equation (59), the midzone stress,

$$\lambda_2 = \left[1 - \frac{1}{SF}\right] F_R . \tag{61}$$

shows that using a conventional constant safety factor, the midzone range will increase as the selected material strength F_R increases. Increasing the resistive stress decreases the tail interference and, therefore, decreases the probability of failure while decreasing the operational elastic range. To maintain a constant midzone stress, while selecting different materials with different strengths, the safety factors would have to change accordingly,

$$SF_2 = \frac{F_{R1}}{F_{R1} - F_{R2}\left[1 - \frac{1}{SF_1}\right]} . \tag{62}$$

This is no surprise. The original safety factor of 1.5 was based on the ultimate and yield stress ratio of aluminum used in the late 1930's. The compromise on 4130 steel was acknowledged and accepted at that time[23] because of its limited usage on aircraft. Current NASA minimum safety factors are 1.4 on design ultimate, a minimum of 1.0 on design yield, and a 1.4 qualification test factor on all metallic structures. High-strength steels are now extensively used on solid rocket booster cases, and figure 17 depicts the relative elastic stress performance denied the case membrane (darkest bars) using current safety factors based on ultimate stress.

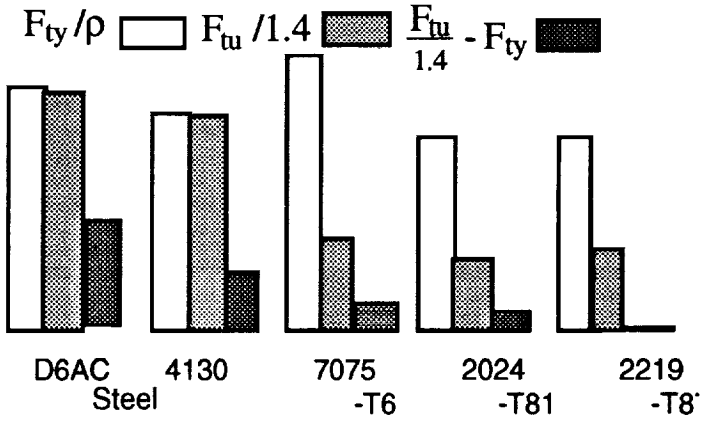

Figure 17. Safety factor relative effects.

This resulting excessive elastic stress margin on a steel motor case membrane cannot be rationalized as improving the rocket motor reliability. The case membrane thickness is usually dominated by the hoop stress induced by the well-defined maximum expected combustion pressures, which amply accommodates all longitudinal stresses induced by thrust and other ascent trajectory environments. Moreover, motor case abnormal critical failure modes are due to joint leakage, case burn-through, and uncontainable combustion pressure spike caused by propellant grain cracks, none of which can be prevented by increased thickness margins. Figure 17 further illustrates that a stress audit indicting a steel structure with a negative safety margin in the midzone may have more reserved (denied) elastic margin than some aluminum structures with positive margins. Figure 12 also reveals that steels contain more inelastic resistance than aluminums for anomalous loads backup.

As long suspected, the current evaluation of structural integrity based on the deterministic method is extraneously arbitrary and incomplete. Of course a higher safety factor provides a more reliable structure than a lower factor, but not necessarily if the lower safety factor structure is A-based and the design load probability is higher, equation (58). An arbitrarily and independently selected high limit load probability would seem to provide a safer structure than one with a lower probability, but not if the combined load and material strength standard deviation is larger than the limit load with a lower probability and a much lower combined standard deviation, equation (57). Hence, it follows that a uniformly safe structural system should combine all the designer control parameters and given standard deviations into a unified standard or criterion. There are usually physical and economic realities for developing unified standards and obligating interface control parameters which, as pursued, contribute to a more rational, enduring, and complete system analysis.

No change in the present deterministic stress audit practice is suggested here, but an independent critical system safety criterion, which integrates loads, stress, and material safety contributions, is obviously wanted. Such a criterion should provide a system standard to complement the deterministic stress audit, avoid the costs of redesign and reverification of an otherwise safe structure, and avoid the cost of a flight structural failure or the blind risk of operating a marginally structural system.

A frequent misuse of the safety factor is to assume that it includes uncertainties. The current NASA criterion specifies a 1.4 design factor on ultimate and a 1.4 factor on verification, which clearly does not allow test negative margin for structural uncertainties as before. All uncertainties must now be estimated and appropriately applied to all structural forms analyses. Their purpose is to be sacrificed during test by the real hardware response without reducing the guaranteed 1.4 safety factor.

B. Uncertainties

It has been wisely said that rough estimates of uncertainties are not the main cause of frequent verification failures, but the total neglect of them is. Identifying unusual and recurring structural uncertainty sources, estimating not too large or too small allowances, and appropriately implementing them into the design analysis are essential integrity tasks.

For simplicity and expediency, design iteration phases often use mean value data, and applying design dispersions is postponed. When dispersions and uncertainties are estimated to be significant, they may be ultimately implemented into the deterministic or reliability methods. Uncertainties that are frequently neglected and that most often depreciate the structural integrity are the modeling

uncertainties. There are four basic types of modeling uncertainties: loads, stress, materials, and manufacturing. Combined predicted and modeling uncertainty loads are the test applied loads. Stress, materials, and manufacturing combined with modeling uncertainties are the test article response stresses. These latter three uncertainties are lump verified as either exceeding or diminishing the predicted safety factor.

Stress modeling with most FEM commercial codes can be as accurate as the smallest grid size practical and the competence of the analyst to model the structure and interpret its results. The larger the grid size, the stiffer is the structure and the more optimistic is the stress response, though the less machine time is required. The FEM uncertainty comes down to the sensitivity of the stress convergence to an exact solution and whether the exact solution can be tested. Since this uncertainty is not a dispersion about the applied stress mean, it biases the mean and must be applied as a factor to the applied stress.

Modeling manufacturing uncertainties are judged on available data base and related experiences. Some estimates may be modeled from assumed tolerance behavior. Dynamic loads are decisively dependent on structural stiffnesses which are contingent on material properties dispersions and on manufacturing and assembly tolerances. As discussed before, specified fastener tolerances may be statistically distributed, from which their distributed loading and contact displacements may be modeled and stiffness uncertainty estimated.

Dimensional buildup and final assembly force-fits may produce preloads in operationally critical stress regions. Locked-in stresses are common on highly complex and redundant structures, leading to alternate load paths producing uncertain and inefficient stiffness and load resistances. Contact wear increases tolerances and reduces stiffness with increasing usage. Manufacturing processes are other sources of uncertainties related to shaping, heat treatment, etc., which alter the material mechanical behavior and limits. Margins for uncertainty dispersions caused by known manufacturing and handling defects on high-risk, high-cost structures should be considered to avoid rework and rejects. The list of uncertainties may seem endless, but those assessed to be probable and significant must be incorporated into the analysis. It should be cautioned that incorrect assumptions, faulty software, and other errors and incomplete analyses are amendable and should not be categorized as uncertainties.

Standard deviations uncertainties are combined in conformance with error propagation laws, equations (6) and (7). This type of uncertainty is usually associated with stress and manufacturing dispersions and is combined with the applied stress coefficient of variation derived from response analysis, equation (22). Neglecting it effectively reduces the response standard deviation,

$$\eta_{Ae} = 2\eta_A - [\eta_A^2 + \eta_e^2]^{0.5} \quad . \tag{63a}$$

A similar expression may apply to postponed resistive stress dispersions. Uncertainties that bias the statistical mean must be included as an accumulated uncertainty factor, and random uncertainties may be root-sum-squared and accumulated,

$$e = e_1 + e_1 + e_2 + \ldots [e_k^2 + e_{k+1}^2]^{0.5} \ldots + e_n \quad . \tag{63b}$$

The accumulation factor reduces the allowable applied stress by $F_R = -(1+e)\, F_A$ which opposes the conventional safety factor.

C. System Reliability

It was concluded earlier that the deterministic method did not completely evaluate the integrated system safety which should include reliabilities of loads and material. The deterministic method was also noted to compromise operational performance of high specific strength materials. However, the deterministic method does provide a verification technique, and the first order reliability concept does offer a more comprehensive system safety assessment. Combining the best features of the two methods should provide the desired deterministic reliability criteria based on probability principles to complement stress audits and to support structural risk assessments.

In designing to a specified minimum reliability, the associated safety index of equation (57) must be expressed with design passive and control parameters raised in earlier sections that statistically characterized the applied and resistive stress distributions. The stated limits defined by the conventional safety factor of equation (60) imply a probability nature which is specified by tolerance limit, equations (8b) and (33), developed from loads and materials interface analyses and are rewritten, respectively,

$$B = \frac{F_A}{\mu_A} = (1+N_A\eta_A)\,, \qquad A = \frac{F_R}{\mu_R} = (1-K\eta_R) \quad , \tag{64a}$$

to simplify their presentation and repeated applications. The applied stress tolerance limit factor is adjusted to include propagation uncertainties of equation (63a) and is expressed by

$$B_e = (1+N_A\eta_{Ae}) \quad . \tag{64b}$$

Substituting the means from equations (64a) tolerance limits into λ_1 and λ_3 zones, the mid zone from equation (59), and the relationship of equation (60) into equation (58), defines the numerator of the safety index as

$$u = \varphi SF\,(1+N_A\eta_A) - (1-K\eta_R) + (\varphi SF-1)(1+N_A\eta_A)\,(1-K\eta_R) \quad . \tag{64c}$$

Substituting standard deviations from equations (64a) and relationship of equation (60) into the safety index denominator and combining into equation (57) provides the safety index equation of the deterministic reliability method,

$$Z = \frac{\varphi SF\,(1+N_A\eta_A) - (1-K\eta_R) + (\varphi SF-1)\,(1+N_A\eta_A)\,(1-K\eta_R)}{\left[(\varphi SF)^2\,\eta_R^2\,(1+N_A\eta_A)^2 + \eta_A^2\,(1-K\eta_R)^2\right]^{\frac{1}{2}}} \quad , \tag{65a}$$

or

$$Z = \frac{\varphi SF\,B - A + (\varphi SF-1)\,BA}{\left[(\varphi SF)^2\,\eta_R^2 B^2 + \eta_A^2 A^2\right]^{\frac{1}{2}}} \quad . \tag{65b}$$

The safety index is applicable to either yield or ultimate failure modes of polycrystalline materials. While there is no condition on its application to a yield failure mode, a safety factor applied on the ultimate failure mode must comply with

$$SF \geq \frac{F_{tu}}{F_{ty}} ,$$

to assure that the structure does not operate through the inelastic region of metallic materials as illustrated in figure 16. The recently specified NASA safety factor criterion on ultimate stress satisfies that condition for most metallics.

Once the minimum safety index is specified for yield or ultimate failure mode in a given structural region, the application of design parameters into equation (65) is essentially the integration of factors developed in earlier interface discipline discussions. The safety factor, SF, is prescribed by the NASA unified safety factor criteria. The material is selected from section V considerations and the A- or B-basis chosen for the failure mode, all of which specify the resistive stress tolerance limit factor $(1-K\eta_R)$ and its characteristics. The applied stress tolerance limit factor $(1+N_A\eta_A)$ was derived from the response analysis and characterized by equations (23) and (33). These are passive and designer control parameters, and are currently independently derived. Though the control parameters N_A and K may be used to fine tune equation (65a) to the specified reliability and safety factor, a more expedient and direct approach is to control the safety index through a modified safety factor "$\phi\, SF$" solved from equation (65b),

$$\varphi\, SF = \frac{A}{B}\left\{(B+1)(A+1)+\left[((B+1)(A+1))^2-((1-Z^2\eta_R^2)+A(A+2))((1-Z^2\eta_A^2)\right.\right.$$

$$\left.\left.+B(2+B))\right]^{\frac{1}{2}}\right\} \div \left\{(1-Z^2\eta_R^2)+A(A+2)\right\}. \qquad (66)$$

The design application of the deterministic reliability method is thus reduced to determining the modified safety factor, $\phi\, SF$, and applying it to stress analyses in lieu of the conventional safety factor. Since the safety index, safety factor, and material are constant for a structural component, the only changes required of equation (66) for calculating the modified safety factor from one region to another is the response standard deviation. The method generates a uniformly reliable structure, and its application requires no new skills or more exceptional understanding and effort than the conventional safety.

However, equation (66) does not include propagation and cumulative design uncertainties. Combining the propagation errors with the applied stress dispersions, compensating the mid zone, λ_2, for the cumulative error as discussed, and retaining all other parameters in equation (65), a constant safety index is satisfied by

$$Z = \frac{(\varphi_D\, SF)B_e - A + AB_e((\varphi_D\, SF) - e - 1)}{\left[\eta_R^2(\varphi_D\, SF)^2 B_e^2 + \eta_{Ae}^2 A^2\right]^{\frac{1}{2}}} , \qquad (67)$$

With a revised "design-to" modified safety factor, $\phi_D\, SF$. Solving for the modified safety factor as before from equation (67), the design safety to be applied to stress analyses is

$$\varphi_D SF = \frac{A}{B_e}\left\{(B_e(1+e)+1)(A+1)+\left[(B_e(1+e)+1)(A+1))^2-((1-Z^2\eta_R^2)\right.\right.$$

$$\left.\left.+A(A+2))((1-Z^2\eta_{Ae}^2)+B_e(1+e)(2+(1+e)B_e))\right]^{\frac{1}{2}}\right\}$$

$$+\left\{(1-Z^2\eta_R^2)+A(A+2)\right\}. \qquad (68)$$

The acceptance of this proposed deterministic reliability method depends on perceiving an affordable experimental verification method, and on establishing confidence in a minimum allowed safety index standard for a range of aerostructures. The deterministic method currently verifies the applied and resistive stress response through the safety factor relationship of equation (60) which is common to the safety index of equations (65). Therefore, a test verified safety factor by the deterministic method is a representative input to the verification of the deterministic reliability method. However, the modified safety index of equation (68) applies only to design analyses. Since estimated uncertainty parameters are expected to be absorbed by the authentic characteristics of the test structure, the net verified safety index Z_T must exclude these sacrificial parameters in equation (67) and must include the safety factor coefficient of equation (66) and the test derived safety factor SF_T from deterministic tests,

$$Z_T = \frac{\varphi SF_T B-A+AB(\varphi SF_T-1)}{\left[\eta_R^2 \varphi SF_T^2 B^2+\eta_A^2 A^2\right]^{\frac{1}{2}}}, \qquad (69)$$

for $e = \eta_e = 0$ test condition.

Confidence in the proposed reliability criterion may be established by relating sets of safety index design parameters to representative parameters in prevailing deterministic designs. Excluding design uncertainties, which are task unique, the safety index design criterion should be based on the selection of five typical parameters defining equation (65a). The designer control parameters, SF, K, and N_A and the passive coefficients of variation, η_R and η_A, are developed throughout the system design analyses and are identically applied to the deterministic and safety index methods.

A correlation approach is to examine the range of these five parameters and the safety index sensitivity to them, and then bound the index with combinations having a range of parameters associated with past successful structures based on deterministic methods. Coefficients of variation of most metallic materials range between 0.03 and 0.08. Probability range factors are between 2 and 4. Measured dispersions about the lateral mean loads obtained from nine flights were within 10 percent, the measured axial dispersions were 60 percent less. Common safety factors are 1.0 on the yield failure mode and 1.4 safety factor on the fracture mode.

Applying arbitrary ranges of parameters and combinations into equation (65a), rough order sets of minimum safety indexes were exceeding 4 on yield and 7 on fracture. It is interesting that current practices using 3-sigma loads and A-basis materials exceed the 9_4 reliability often specified in request for proposals. The 40 percent increase in safety factor nearly doubled the safety index, which touches on the irrelevance of reliability using large safety factors. This nonlinear relationship also asserts that sensitivities must be evaluated for small variations from baselined values. While there is merit in a 9_5's reliability resulting from a safety index based on yield failure, there is little confidence for pursuing a safety index based on large ultimate safety factors.

A coherent approach to evolving a reliability criterion is to assess the sensitivity of the safety index with each parameter and then select parameters from statistical distributions of significant parameters. Expressing the safety index by

$$Z = \frac{u}{v} \ , \tag{70}$$

the numerator and denominator from equation (65a) are defined by

$$u = SF\,(1+N_A\eta_A)-(1-K\eta_R)+(SF-1)(1+N_A\eta_A)(1-K\eta_R) \ , \tag{71a}$$

and

$$v = \left[\eta_R^2\,SF^2(1+N_A\eta_A)^2+\eta_A^2(1-K\eta_R)^2\right]^{\frac{1}{2}} , \tag{71b}$$

respectively. The resulting safety index sensitivities are:

$$\frac{\partial Z}{Z} = B\,SF\left[\frac{1}{u}\,(1+A(SF-1)) - \frac{1}{v^2}\,(\eta_R^2\,B\,SF)\right]\frac{\partial SF}{SF} \ , \tag{72a}$$

$$\frac{\partial Z}{Z} = \eta_A\left[\frac{N_A}{u\,B}\,(SF+A(SF-1) - \frac{1}{v^2}\,(\eta A^2+\eta_R^2\,SF^2B\,N_A)\right]\frac{\partial \eta_A}{\eta_A} \ , \tag{72b}$$

$$\frac{\partial Z}{Z} = -\eta_R\left[\frac{K}{u\,A}((SF-1)B-1) + \frac{1}{v^2}\,(\eta_R\,B^2\,SF^2-\eta_A^2AK)\right]\frac{\partial \eta_R}{\eta_R} \ , \tag{72c}$$

$$\frac{\partial Z}{Z} = N_A\eta_A\left[\frac{SF}{u\,B} - \frac{1}{v^2}\,(\eta_R^2SF^2\,B)\right]\frac{\partial N_A}{N_A} \ , \tag{72d}$$

$$\frac{\partial Z}{Z} = K\,\eta_R\left[\frac{1}{u\,A}\,(B(SF-1)-1) + \frac{1}{v^2}\,(\eta_R^2A)\right]\frac{\partial K}{K} \ . \tag{72e}$$

Applying the same set of parameters in equations (72) as was used in the previous rough order analysis, sensitivities about the ultimate stress safety factor drove all the parameters to insignificance, as expected, and again suggested basing the safety index on the yield failure mode. Then using yield safety factor of unity, the safety index was determined to be most sensitive to the conventional safety factor and an order of magnitude less sensitive to the control parameters N_A and K. It seemed helpful that the safety index was even less sensitive to the passive parameters η_R and η_A because they are the limited observed or derived data base. It became clear that a safety index criterion development would anchor the yield safety factor and select probable $K\eta_R$ and $N_A\eta_A$ products from statistical distributions of A-basis materials and typical loads forcing functions respectively. This study is the subject of another paper.[24]

Indexing on the yield failure mode should be favored,[25] not only because of its compatibility with reliability as required to support risk analyses, but just as importantly, because the primary purpose of a robust structure is to assure that all nominal operating loads are sustained elastically.

That primary operating purpose should not be compromised by low risk or overstated contingencies. Any material resistance beyond yield is arbitrarily reserved for special and abnormal conditions and for unpredictable phenomena within the NASA ultimate safety factor criteria. Exceeding the operating elastic limit may provide a fail-safe condition for that structure and area, but exceeding the elastic stress region to fracture may not allow it to fail operationally, and it may not prevent downstream failure of other critical structural areas, joints, and seals. However, indexing on yield raises the issue of acceptable verification.

In applying the safety index to the yield failure mode, yield predictions are based on more accurate linear analytical and computational methods than nonlinear ultimate failure methods. Further, the much smaller system safety index produces shorter overlapping distribution tails having more realistic data content. In fact, applying the NASA 1.0 safety factor on yield stress would reduce the mid-zone of equations (59) and (58) and figure 14 to $\lambda_2 = 0$, all of which would degenerate the deterministic reliability index into the conventional first order reliability concept.

Therefore, in experimentally determining the safety factor by the current deterministic method of equation (60), and then substituting it into equation (69), the first-order reliability is experimentally verified according to the substituted experimental safety factor exceeding or receding from the factor of one. This is an interesting discovery, because now the deterministic reliability technique is provided with a timely and economical method for verifying the conventional first-order yield reliability of semistatic structures to the same standard as the conventional deterministic method.

Though yield stress prediction may be more accurate than the ultimate stress, the exact location of its initiation on the test structure is difficult to detect for reasons already discussed in section V. The inaccuracy should be particularly negligible in using linear FEM model predictions to track it. Nevertheless, the reliability method does provide an absolute probability insight for assessment and modification decisions. On the other hand, missing the experimental yield in the deterministic method provides very limited information for evaluation, since test-derived safety factors are relative and ignore the safety contributions of the applied loads and material probabilities.

In applying the safety-index criterion on the ultimate failure mode, the predicted fracture point and applied load accuracy would be limited by the formidable nonlinear analysis, available supporting data, and plastic strain history. However, the location and nature of fractures are more accurately determined and correlated to the test fracture load and more becoming to the deterministic method. But again, it represents one fracture data point with little decision making clues for the probable outcome of other articles. Though the current deterministic method has many weaknesses that may be easily surmounted by the first-order reliability method, it requires some shift in analysts' notions and development of confidence. Prevailing deterministic static test criteria accommodate either methods.

VII. QUALITY FUNCTIONS

In a genuine competition for limited resources, the incentives are to experiment in producing a best-suited product for the changing environments, and to build it with quality functions. In this context, all customary design notions must be challenged and vitalized in response to pressing changing environments. A quality function concept in a changing environment may be framed from

quality function development[26] (QFD) by designing products with features critical to today's manufacturing and service sectors. Changed features must be based on studies of past practices and results to provide better quality than the original product and with reduced lead time.

Where the carrier developer and user are one, life-cycle cost with emphasis on initial and recurring costs is the design reigning controller. Based on current operational experiences, what structural requirements difference should be imposed on expendable versus reusable carrier elements to minimize production and operational costs? Considering traffic models, cost of inventory, and consequence of risk, are there structural criteria differences on manned versus unmanned carriers that cannot be economically incorporated into common launch stages? Formulating (off-line) these and other upper tier structural design criteria to changing customer voices, technologies, and resources should benefit conceptual development at the highest quality leverage.

The demand for affordability and the gravity of cost overrun should blend cost training and estimators into the design staff for more timely and tenable monitoring and modifications. Increasing cost of continuously updating computational equipment and skills, and jumbo programming should increase performance, reliability, development, production, and operational payoffs. Design analysis should deliberately strive to maximize that payoff.

Quality functions which improve reliability over a wide range of conditions and are user friendly through all downstream events have been touched in preceding sections. They are briefly generalized in the following sections to impress their importance and inferred persuasion that they should be innovated into structural product design analyses of interacting interfaces.

A. Performance

A changing environment in performance is the public's growing antipathy to launch pad glitches and postponements. The appeal of space events is adventure, but launch is becoming a less rousing one. After a quarter-century development of carrier technology, it is becoming more difficult to not count aerospace carriers as a matured industry. The dare-and-do missions of the past have graduated into present commercial markets and competition. Cutting-edge performance has given way to least cost and reliability priorities.

Though structures have had the least share of development and operational problems, it can do better. Reference 27 is one of Mr. Robert Ryan's many publications on lessons learned and related structural topics to avoid repetitions. With increasing structural complexity and performance and with limited senior staffs, perhaps more effort should be shifted to exploring more and new potential failure sources and less to excessive programming of well established failure modes with obvious solutions.

Catastrophic structural failures of heavy and expensive launchers can be avoided with some creativity and little cost. Polycrystalline structures have one primary operational failure mode and an abnormal fracture mode. A third postfracture safe mode may sometimes be crafted by guiding the load paths of the fractured structural article to sustain the fractured load level and more. The solid booster aft skirt supporting the entire shuttle assembly on the launch platform has demonstrated this feature by test. Critical pressure vessels may be designed to "leak before burst" through inelastic and material design techniques. Failure mode and effect analysis (FEMA) might be more effective if activated in early design phases to determine how the safe failure of one structural part would fail another part, probability of occurrence, criticality, and how they might be prevented or minimized.

Development and selection of structural solutions and options are the most important design functions in fixing operational, reliability, and cost characteristics into a product's total life cycle. The cost of modifying an operational structural system to improve traffic and reduce recurring costs is magnified by related modification to supporting facilities at the worst quality leverage phase. Relying on concurrent engineering alone to consistently select the best life-cycle option during design phases is too chancy. A supporting progressive guide is coveted. Pugh compares one option against another and enhances them in the process. The technique uses a matrix of criteria versus options for complete visibility. One option is used as a datum and others are compared and graded with plus or minus compliance with criteria. All evaluated options are reviewed and modified to pass the criteria. Weak ones are eliminated until one strong concept persists.

New starts, turnovers, and influx of new personnel are a continuous change in the industry. Designers should no longer presume that development, production, and operations will be supervised and executed by the highest skilled using their consistent best effort, and through extensive procedures. Foolproof concepts must be introduced in critical manufactured structural parts, assemblies, joints and seals, and all changeout interfaces. The automobile industry realized production and repair savings and goodwill in reducing extraction of broken studs by restricting fasteners on the engine block to not less than half-inch, and by also shortening the wrench leverage. Foolproof design concepts of parts, production, interfaces, and assembly tools might be incorporated through quality circles and formal design reviews.

B. Manufacturing

Manufacturing equipment, processes, and skills are in a constant state of change, and the vanguard designer keeps abreast through research, seminars, journals, catalogs, site visits, etc. Quality function requires that shape, size, and materials are optimized with manufacturing capabilities and cost in the early design phase. Performance demands are optimized with how it is to be manufactured and how much precision is to be provided.[26]

Processes that meet manufacturing demands are researched, and candidates are selected for least cost or for maximizing precision. Inspection standards are established, and design factors that affect control points and assemblies are identified and optimized through design control parameters. Bottlenecks are also identified and contingencies planned. Most engineering bottlenecks arise when quality targets are set at higher levels than previously experienced and these levels are difficult to achieve. A quality function design integrates and optimizes these manufacturing function interfaces.

C. Verification

Verification is committed to assuring that all design details, performance, and structural integrity comply with specified requirements. Verification may be satisfied through refined analysis of a design final iteration, design similarity of a successfully operating structure, or through experimental testing. Experimental testing is often the most expensive and is the focus of this quality function.

The most significant verification environment changes are the sophisticated computational methods, simulations, and techniques that are constantly evolving to more accurately predict yield and fracture stresses. BEM and many FEM elastic and inelastic commercial codes to resolve global and local stress to failure are extensively and successfully applied. The variety of accomplished operating structures is constantly expanding. All these changes should promote verification by

analysis and similarity and soften the need for routine or broad experimental testing of low-risk systems. Experimental testing should concentrate more on instrumentation and verification of joints and other critical discontinuity stress regions up to fracture.

Commonly stated requirements for experimental testing are to exposure sneak phenomenon or incomplete analysis, to affirm critical failure and post-failure modes, to reveal unique response characteristics, to verify margins and math model response, and to develop inspection procedures. Those requirements that cannot be satisfactorily verified by analysis or similarity should be assessed for their expected experimental result from detailed planning and mock experiment analysis before committing to test. It should be recognized that structural tests provide only limited surface data that must be correlated with a refined math model to completely verify yield and fracture stresses. Fracture modes should be further evaluated through the metallurgical features of the parted surface.

Tests whose boundaries and operational environments are difficult to simulate may also yield results that are difficult to interpret to verify performance. Tests may be performed to failure or to no-failure. A no-fail test provides limited experience no matter how successfully it operates thereafter. A protoflight test, field or flight tests are all no-fail tests and are viable options to experimental testing. Experimental verification is costly, approaches are often hybrid, and worth may be arbitrary. Developing coherent technical and economic guidelines compatible with changing verification environments should be a noble challenge.

VIII. CONCLUSIONS

An aerospace program consists of many interacting systems of which structures was the subject of this study. As in any multitiered, multidisciplined system, the behavior designed into one part by one discipline affects the behavior of other disciplines and parts. The purpose of this study was to optimize the total system performance integration with reliability, development, and least cost through their interactions and interfaces, and to identify interface deficiencies.

The structural system was partitioned into five major performance and three life-cycle disciplines. Their interface designer-controlled parameters were identified by stepping through the system design analysis and understanding discipline interactions and their interface input-output processes. Envelope size and operating environments are usually derived from requirements of mission interacting systems which initiate the structural design process. Material properties were noted to be the hub of all discipline interfaces. Integrity was the balance between delivery performance and reliability. Shaping, dimensioning, and precisioning are the total integration of all disciplines and the net product of a structural part and assembly. Cost is the reigning consideration at all interfaces for a robust total system.

Interface designer-control parameters identified in interdiscipline input-output data must be optimized with delivery performance, reliability, and cost. Once the material is selected, the most significant designer control parameters are shapes, dimensions, and probability range factors. Common practice is to arbitrarily control parameters by the input data disciplines independently of subsequent user disciplines. Concurrent engineering may improve these interface optimizations piecewise, but Taguchi techniques might provide a more coherent and methodical approach.

Stress audit based on current deterministic method was discovered to be incomplete and suspect of inconsistent safety evaluation results. A high safety factor may seem to provide a safer structure than a lower factor, but not necessarily if the lower safety factor structure is designed with higher reliability loads and materials. Applied loads with higher specified probability range may not be safer than lower probability range loads having a lower combined standard deviation of loads and material strength. A deterministic reliability method is proposed to evaluate the total structural safety and to complement the current deterministic stress audit. The combined evaluations may improve the acceptance or rejection criteria of experimental structural results.

The study was limited to carrier structural systems, which are distinguished from other systems by environments and, to a lesser extent, by materials. However, the procedure may be extended to payloads, surface transportation, and high performance structures with similar goals and expectations using their unique space or field environments.

REFERENCES

1. Anon: "Project Management Handbook." MM 7120.2A, NASA Marshall Space Flight Center, AL, June 1989.

2. Meyer, Stuart I.: "Data Analysis." John Wiley & Sons, Inc., New York, NY, 1975.

3. Anon: "Metallic Materials and Elements for Aerospsace Vehicle Structures." MIL-HDBK-5F, 1990.

4. Pugh, S.: "Total Design." Addison Wesley Publishers, Wokingham, England, 1990.

5. Ryan, R.S.: "Structural Margins Assessment Approach." NASA TM-100332, MSFC, AL, June 1988.

6. Craig, R.R.: "Structural Dynamics." John Wiley & Sons, New York, NY, 1981.

7. Eldridge, J.: "Coupled Loads Analysis for Space Shuttle Payloads." NASA TM-103581, MSFC, AL, May 1992.

8. Klein, M., Reynolds, J., and Ricks, E.: "Derivation of Improved Load Transformation Matrices for Launcher-Spacecraft Coupled Analysis, and Direct Computational Margins of Safety." International Conf., Space Structures and Mechanical Testing, Noordwijk, The Netherlands, October 19–21, 1988.

9. Miller, I. et al.: "Probability and Statistics for Engineers." Prentice Hall, Fourth Edition, Englewood Cliffs, NJ, 1990.

10. Phadke, M.S.: "Quality Engineering Using Robust Design." Prentice Hall, Englewood Cliffs, NJ, 1989.

11. Lovingood, J.A.: "A Technique for Including the Effects of Vehicle Parameter Variation in Wind Response Studies." NASA TM X-53042, MSFC, May 1, 1964.

12. Kapur, K.C., and Lamberson, L.R.: "Reliability in Engineering Design." John Wiley & Sons, New York, NY, 1977.

13. Timoshenko, S.P., and Goodier, J.N.: "Theory of Elasticity." Third edition, McGraw-Hill Book Co., NY, 1987.

14. Prager, W., and Hodge, G.: "Theory of Perfectly Plastic Solids." John Wiley & Sons, New York, NY, 1952.

15. Dieter, G.: "Mechanical Metallurgy." McGraw Hill, New York, NY, Third print, 1986.

16. Wilson, C.D.: "Linear Elastic Fracture Mechanics Primer." NASA TM-103591, July 1992.

17. Osgood, C.C.: "Fatigue Design." Second Edition, Pergamon Press, New York, NY, 1982.

18. Verderaime, V.: "Plate and Butt-Weld Stresses Beyond Elastic Limit, Material and Structural Modeling." NASA TP-3075, January 1991.

19. Bruhn, E.: "Analysis and Design of Flight Vehicle Structures." Jacobs Publishing, Inc., Indianapolis, IN., 1973.

20. Ryan, R.S., and Townsend, J.S.: "Application of Probabilistic Analysis/Design Methods in Space Programs: The Approach, The Status, and The Need." 34th AIAA/ASME/ASCE/AHS/ASC Conference, La Jolla, CA, April 19–22, 1993.

21. Neal, D.M., Matthew, W.T., and Vangel, M.G.: "Model Sensitivities in Stress-Strength Reliability Computations." Materials Technology Laboratory, TR 91-3, Watertown, MA, January 1991.

22. Anon: "Structural Design Criteria Applicable to a Space Shuttle." NASA SP-8057, January 1971.

23. Shanley, K.C.: "Historical Note on the 1.5 Factor of Safety for Aircraft Structures." J. of Aerospace Sciences, vol. 29, February 1962.

24. Verderaime, V.: "First Order Reliability Criteria Development Bearing Deterministic Practices." NASA TP to be published.

25. Verderaime, V.: "Aerostructural Safety Factor Criteria Using Deterministic Reliability." J. of Spacecraft and Rockets, vol. 30., No. 2, March–April 1993.

26. Akao Yoji et al.: "Quality Functional Deployment." Productivity Press, Cambridge, MA, 1990.

27. Ryan, R.S.: "The Role of Failure/Problems in Engineering: A Commentary on Failures Experienced—Lessons Learned." NASA TP-3213, March 1992.

☆ U.S. GOVERNMENT PRINTING OFFICE 1993–533-108/80151

REPORT DOCUMENTATION PAGE

Form Approved
OMB No. 0704-0188

1. AGENCY USE ONLY *(Leave blank)*	2. REPORT DATE	3. REPORT TYPE AND DATES COVERED
	November 1993	Technical Paper

4. TITLE AND SUBTITLE
Total Systems Design Analysis of High Performance Structures

5. FUNDING NUMBERS

6. AUTHOR(S)
V. Verderaime

7. PERFORMING ORGANIZATION NAME(S) AND ADDRESS(ES)
George C. Marshall Space Flight Center
Marshall Space Flight Center, Alabama 35812

8. PERFORMING ORGANIZATION REPORT NUMBER
M-733

9. SPONSORING/MONITORING AGENCY NAME(S) AND ADDRESS(ES)
National Aeronautics and Space Administration
Washington, DC 20546

10. SPONSORING/MONITORING AGENCY REPORT NUMBER
NASA TP-3432

11. SUPPLEMENTARY NOTES
Prepared by Structures and Dynamics Laboratory, Science and Engineering Directorate.

12a. DISTRIBUTION/AVAILABILITY STATEMENT
Unclassified—Unlimited
Subject Category: 15

12b. DISTRIBUTION CODE

13. ABSTRACT *(Maximum 200 words)*

Designer-control parameters were identified at interdiscipline interfaces to optimize structural systems performance and downstream development and operations with reliability and least life-cycle cost. Interface tasks and iterations are tracked through a matrix of performance disciplines integration versus manufacturing, verification, and operations interactions for a total system design analysis. Performance integration tasks include shapes, sizes, environments, and materials. Integrity integrating tasks are reliability and recurring structural costs. Significant interface designer control parameters were noted as shapes, dimensions, probability range factors, and cost. Structural failure concept is presented, and first-order reliability and deterministic methods, benefits, and limitations are discussed. A deterministic reliability technique combining benefits of both is proposed for static structures which is also timely and economically verifiable. Though launch vehicle environments were primarily considered, the system design process is applicable to any surface system using its own unique filed environments.

14. SUBJECT TERMS	15. NUMBER OF PAGES
structural design, analysis, optimization, interfaces, integrity, reliability, materials, safety factor, dynamics, parameters, quality, system, sensitivities; launch vehicles	67
	16. PRICE CODE A04

17. SECURITY CLASSIFICATION OF REPORT	18. SECURITY CLASSIFICATION OF THIS PAGE	19. SECURITY CLASSIFICATION OF ABSTRACT	20. LIMITATION OF ABSTRACT
Unclassified	Unclassified	Unclassified	Unlimited